DEMOCRATIC REPUBLIC OF ALGERIA
وزارة التعليم العالي والبحث العلمي
MINISTRY OF HIGHER EDUCATION AND SCIENTIFIC RESEARCH
جامعة عمار ثليجي بالأغواط
AMAR TELIDJI UNIVERSITY, LAGHOUAT
كلية التكنولوجيا
TECHNOLOGY FACULTY
قسم الكترونيك
ELECTRONIC DEPARTEMENT

Master Thesis

In view of obtaining the Master's degree

Science and Technology Field

Electronics Sector

Option: Instrumentation

Theme

SIMULATION AND CONCEPTION OF MIMO BIOSENSOR FOR DAMAGE LUNGS RUNG CLASSIFICATION.

Submitted by:

Derar Rania

Supervised by:

Pr. DJERFAF Fatima

Members of the Jury:

Mrs. CHOUIREB Fatima	University of Laghouat	President
Mr. BENSAFEDDINE Jalalelddine	University of Laghouat	Examiner
Mrs. DJERFAF Fatima	University of Laghouat	Supervisor

2023/2024

Abstract

In the aftermath of the COVID-19 pandemic, many individuals have suffered from severe health repercussions, including both short and long-term lung damage. While X-rays have traditionally been employed for detecting lung issues, the need for faster and more efficient diagnostic methods is evident. In response to this need, this study introduces a novel split ring resonator (SRR) as Multiple-Input Multiple-Output (MIMO) biosensor. It is designed for the millimeter range, to swiftly and safely detect pneumonia associated to the COVID-19. Operating within the 5G frequency bands (36 GHz to 38 GHz) and leveraging metamaterial technology, this biosensor offers a compact solution for identifying lung abnormalities. By analyzing the water percentage in the lungs, the MIMO biosensor distinguishes the lung damage's levels. Through extensive neural network classification and MIMO biosensor's S parameters, a robust model for accurately classifying lung damage is developed. The proposed MIMO biosensor device demonstrates precise detection of affected lung level.
Keywords: Biosensors, MIMO device, Metamaterials, Neural networks, COVID-19, Lungs.

Résumé

Suite à la pandémie de COVID-19, de nombreux cas pulmonaires, nécessitant des méthodes de détection rapides et efficaces que les rayons X traditionnels. Cette étude propose un nouveau biocapteur MIMO à métamatériaux et à résonateur à anneau fendu pour détecter rapidement la pneumonie liée au COVID-19. Fonctionnant dans les bandes de fréquence 5G, ce biocapteur MIMO permet une détection précise des anomalies pulmonaires en quantifiant le pourcentage d'eau dans les poumons. Grâce à une classification neuronale et les parametres S de biocapteur MIMO, un modèle robuste de classification est développé, offrant ainsi un outil prometteur pour améliorer les diagnostics les rangs des poumons affectés.
Mots-clés : Biocapteurs, COVID-19, MIMO, Métamatériaux, poumons, réseaux de neurones.

ملخص

بعد جائحة COVID-19، حدثت العديد من حالات تلف الرئة، مما يتطلب طرق اكتشاف أسرع وأكثر فعالية من الأشعة السينية التقليدية. تقترح هذه الدراسة حساس رنان MIMO حلقي مشقوق للكشف بسرعة عن الالتهاب الرئوي المرتبط بـ COVID-19.يعمل هذا الحساس في نطاقات تردد 5G مع المواد الخارقة، ويسمح بالكشف الدقيق عن تشوهات الرئة عن طريق تحديد نسبة الماء في الرئتين.

من خلال تصنيف الشبكة العصبونية ومحاكاة العوامل S للحساس ، تم تطوير نموذج فعال لتصنيف إصابات الرئة، مما يوفر جهاز سريع واعد لتحسين تشخيص الرئة المصابة.
الكلمات المفتاحية: COVID-19 ، المستشعر الحيوي، MIMO، مواد الخارقة، ، الرئة، الشبكة العصبونية.

Acknowledgements

Alhamdulillahirabbil'alamin, praise to Allah, The Most gracious, and the Most Merciful. Praise to Allah for the blessings endowed to me so that I can accomplish this piece of work entitled "Simulation and conception of MIMO biosensor for damage lungs rung classification" as the requirement for getting the Master's degree of Instrumentation of Amar Telidji University of Laghouat.

I would like to express my sincerest gratitude to Pr. F. Djerfaf my thesis supervisor, for her patient guidance during the process of writing this thesis. Her invaluable comments and suggestions have led to numerous improvements of my thesis.

I would also like to thank Mr. Mohammadi Naili for his time and help in fabricating the sensor.

Last but not least my special appreciation to my family and friends. To all of them I dedicate this piece of work. Thanks also to all of my classmates for togetherness, kindness, and motivation.

I welcome constructive comments and suggestions from readers to further improve this thesis. I hope it will be valuable to those interested in advancing biomedical applications.

Dedication

*Appreciatively, I dedicated this thesis to **ME**, another part of myself that always eager for challenges in life. And especially for:*

My beloved parents. Thank you so much for everything! Words can hardly describe my thanks and appreciation to you. You have been my source of inspiration, support, and guidance. You have taught me to be unique, determined, to believe in myself, and to always persevere. I am truly thankful and honored to have you as my parents.

My sister Sara & brother Mohamed Yacine who always cheer me up, words can never express my deep love and gratitude to them. May Allah always give them health and always take care of them.

My beloved best friend since elementary school Chaima & All my best friends and family.

My roommate friend who always support me Sondos.

All those who have helped the researcher to complete the thesis which may not be mentioned one by one.

To all those I love and those who loves me.

TABLE OF CONTENT

LIST OF FIGURES

List of figures

LIST OF TABLES

LIST OF ABBREVIATIONS

MIMO	Multiple input and multiple output
COVID-19	Corona virus disease-19
SARS	Severe Acute Respiratory Syndrome
ARDS	Acute Respiratory Distress Syndrome
MRI	Magnetic Resonance Imaging
DNA	Deoxyribonucleic Acid
CEA	Carcinoembryonic Antigen
EGFR	Epidermal Growth Factor Receptor
FET	Field-Effect Transistor
SRR	Split Ring Resonators
ANN	Artificial Neural Network
Tansig	Tangent sigmoid
SVM	Support Vector Machine
AdaGrad	Adaptive Gradient Algorithm
BP	The Backpropagation algorithm
LEARNGDM	Gradient Descent with Momentum
SoftMax	Soft Maximum
MSE	Mean Squared Error

GENERAL INTRODUCTION

The COVID-19 pandemic has triggered global alarm within the healthcare sector, resulting in devastating losses of lives, economic downturns, and disruption of daily life. The highly contagious nature of the virus has wreaked havoc worldwide, prompting extensive efforts to comprehend its complexities. Clinical manifestations vary widely, with fever, cough, and fatigue and damage lungs being the most prominent symptoms. Other less common symptoms include congestion, runny nose, sore throat, and diarrhea. The challenge lies in navigating the unpredictable clinical course, which can lead to severe complications. Pneumonia and acute respiratory distress syndrome (ARDS) are among the major short-term and long-term lung complications associated to COVID-19. In pneumonia, the normally air-filled sacs in the lungs become inflamed and filled with fluid, resulting in breathing difficulties and coughing, among other lung ailments. Therefore, the urgent need for effective markers to track disease severity and prognosis is paramount for timely medical intervention.

In recent years, there has been a burgeoning interest in employing artificial neural networks in biosensing for disease detection and diagnosis. In this work, biosensors play a significant role in enhancing the detection of lung damage. The integration of Multiple-Input Multiple-Output (MIMO) technology with metamaterials into biosensors represents a groundbreaking advancement. Notably, the ability to quantify water percentage in the lungs provides crucial insights into the extent of damage lungs.

The study is structured into three core chapters:

Chapter 1 delves into the fundamental concepts of biosensors and their operational principles. Through an exploration of the mechanisms underlying these devices, valuable insights are gained into their myriad applications, particularly in medical diagnostics. Advanced biosensor technologies, including MIMO antenna and metamaterial-based sensors, with a specific focus on leveraging MIMO sensors to enhance the detection of lung damage levels.

Expanding on this foundation, Chapter 2 investigates the integration of neural networks to bolster the performance and reliability of MIMO biosensor biosensors. Leveraging the capabilities of machine learning and pattern recognition, neural networks enhance sensitivity and selectivity by extracting information from intricate biological signals.

Chapter 3 centers on the fusion of MIMO biosensor biosensors with artificial neural networks, achieved through HF simulation and diverse ANN models. The primary objective is to accurately detect and classify varying levels of lung damage. This chapter meticulously presents and scrutinizes all simulation results.

In summary, our study aims to design a 5G MIMO biosensor for detecting lung damage levels by quantifying the water content in COVID-19 patients, this approach aims to develop a robust, non-invasive, and efficient diagnostic tool that can significantly improve early detection and treatment outcomes for patients with lung damage. Subsequent chapters will delve deeper into specific methodologies and results, offering a comprehensive understanding of our research outcomes.

CHAPTER I

BIOSENSORS

I.1 Introduction

This chapter discusses key areas of biosensors, particularly in the context of early lung damage level detection. We begin by elucidating the statement of the problem: lung damage level and emphasizing the urgency for timely detection to improve patient outcomes. Biosensors are proving to be a promising solution and offer the possibility of rapid and accurate detection of damage level markers. We explore their historical evolution, fundamental components, diverse types, and wide-ranging applications spanning healthcare, environmental monitoring, and food safety. While acknowledging their remarkable sensitivity and specificity, we also address the challenges and limitations associated with biosensors. Furthermore, we introduce advanced biosensor technologies such as microwave and metamaterial-based sensors, culminating with the introduction of MIMO sensors as a novel approach to improve the effectiveness of lung damage level detection.

I.2 Statement of the problem

On March 11, 2020, the World Health Organization (WHO) declared the novel coronavirus (COVID-19) outbreak a global pandemic [1]. The impact of COVID-19 in Algeria has been profound, affecting various aspects of life and healthcare. As of the latest update on December 19, 2023, data reported to WHO highlights the current situation in the country. In the last 24 hours, there have been no new cases reported. However, the total number of confirmed cases has reached 272,010, with 6,881 confirmed deaths [2].

COVID-19 severity is associated with the presence of comorbidities such as cardiovascular disease, hypertension, obesity, diabetes, chronic lung disease, and cancer. SARS-CoV-2 mainly causes mild respiratory infections but may also progress to interstitial pneumonia and severe acute respiratory distress syndrome (ARDS), which are most common in older patients. However, it can also affect other organs such as the liver, kidneys, and heart. Importantly, it has been established that COVID-19 can cause severe vascular injury and severe neurological manifestations [3-4].

ARDS occurs when fluid accumulates in the lungs' tiny, stretchy air sacs (alveoli). These fluids prevent your lungs from filling with enough air, which means less oxygen reaches your bloodstream. This deprives your organs of the oxygen they need to function [5]. **Figure I.1** illustrates a comparison between a Normal lung model and a Damaged lung model. The damaged lung phantom was created using skin, fat, muscle, water, and a lung layer, providing

a visual representation of the structural changes and challenges associated with conditions like ARDS.

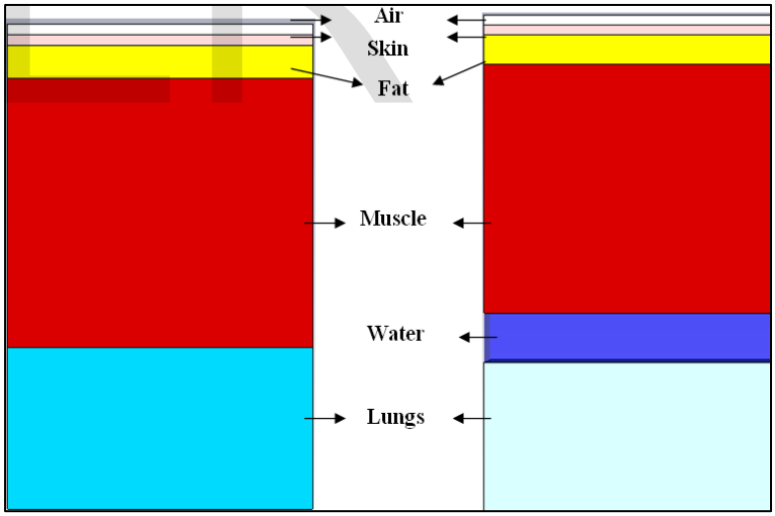

Figure I.1: Normal lung model and Damaged lung model [6].

There are currently no established treatment guidelines for post-COVID lung disease. Initially, corticosteroids were used early in the pandemic to treat persistent lung issues and seemed to help with symptoms and recovery. However, later studies found that corticosteroids might harm hospitalized patients not on respiratory support, leading to caution in their use for outpatients. Antifibrotic drugs like nintedanib and pirfenidone were considered for preventing lung fibrosis after COVID-19, but only nintedanib is still being tested in clinical trials. For severe cases, lung transplants are an option, but they are complex and require careful patient selection despite good short-term outcomes [7].

In this situation, faster detection of affected lung is necessary. Current techniques for detecting lung damage have drawbacks, such as radiation exposure, false negative, and high cost is associated with chest X-ray and computed tomography (CT) scans [8]. While MRI and positron emission tomography (PET) scans are reliable diagnostic tools, they may not be suitable for patients with additional medical complexities [9]. Recent advances in biomedical sciences have enabled cost-effective and efficient assessment of COVID-19 biomarkers using biosensors. These biosensors offer high specificity, selectivity, and affordability, making them ideal for rapid detection. They can quickly identify inflammatory, hematological, immunological, and biochemical markers of COVID-19, helping to reduce patient mortality. Additionally, the development of biosensors and medical devices enhances the detection of infectious diseases and complements other diagnostic tests [10].

I.3 History and definition

The inception of biosensors traces back to 1962 when scientist Leland C. Clark introduced enzyme electrodes. Subsequently, interdisciplinary efforts spanning VLSI, Physics, Chemistry, and Material Science have advanced the development of increasingly sophisticated and reliable biosensing devices. These innovations find applications across various fields including medicine, agriculture, biotechnology, military, and bioterrorism detection and prevention [11].

In a biosensor, the phenomenon is recognized by a biological system called a bioreceptor, which is in direct contact with the sample and forms the sensitive component of the biosensor. The bioreceptor has a particularly selective site that identifies the analyte [12].

I.4 Design and principle

A proficient biosensor comprises two primary elements: a biological receptor or sensor element and a transducer. A signal processing unit that usually contains a display or printer is normally used in conjunction to a biosensor as depicted in **Figure I.2** [13].

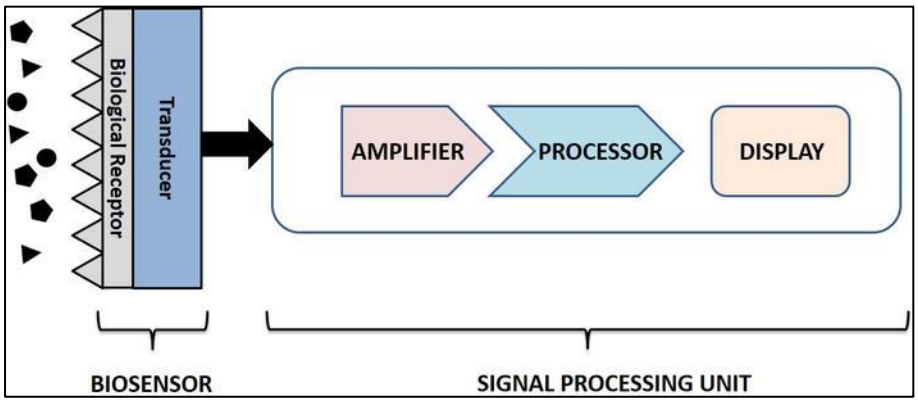

Figure I.2 : Biosensor design showing the various components necessary for generating a signal [13].

Biological receptor: This pivotal element, sometimes denoted as a sensor or detector unit, holds significant importance in detecting and quantifying the concentration of the target analyte [14]. Serving as a biological receptor, it exhibits specific recognition of the target analyte, initiating a signal in the form of light, heat, pH, charge, or mass alteration upon interaction [15]. The biological receptor must possess high specificity, stability under storage conditions, and be immobilized. It should selectively detect the target compound in the test sample, influencing the device's sensitivity [16]. Examples of this component include tissues, microorganisms, organelles, cell receptors, enzymes, antibodies, or deoxyribonucleic acid (DNA) or ribonucleic acid (RNA), categorized into catalytic and non-catalytic receptors [14].

Catalytic receptors are suitable for continuous monitoring of substances at higher concentrations, while non-catalytic receptors are employed in biosensors for measuring low-concentration analytes, typically in non-reusable devices [17].

Transducer: A transducer, the second primary element in a biosensor, serves as a material capable of converting energy from one from to another [15]. Within a biosensor setup, the transducer's role involves converting the biochemical signal obtained from the biological receptor, arising from the interaction between the target analyte and the biological receptor, into a quantifiable and measurable signal, which may include piezoelectric, optical, or electrochemical signals, among others. The transducer detects and gauges the alteration that occurs during the interaction between the biological receptor and the analyte [18]. When designing a transducer, it's recommended to consider several features such as specificity to the target analyte, analyte concentration range, response time, and practical applicability [13].

In simple words, a biosensor consists of a biological component that helps the device recognize or communicate with the analyte. This interaction elicits a physical or chemical response, which is subsequently captured by a transducer. Utilizing this information, the transducer then converts it into an electrical signal. These signals are then passed on to the electronic (amplifier, processor) to convert it into a readable form. Finally, after all these processes the output is displayed [19-20].

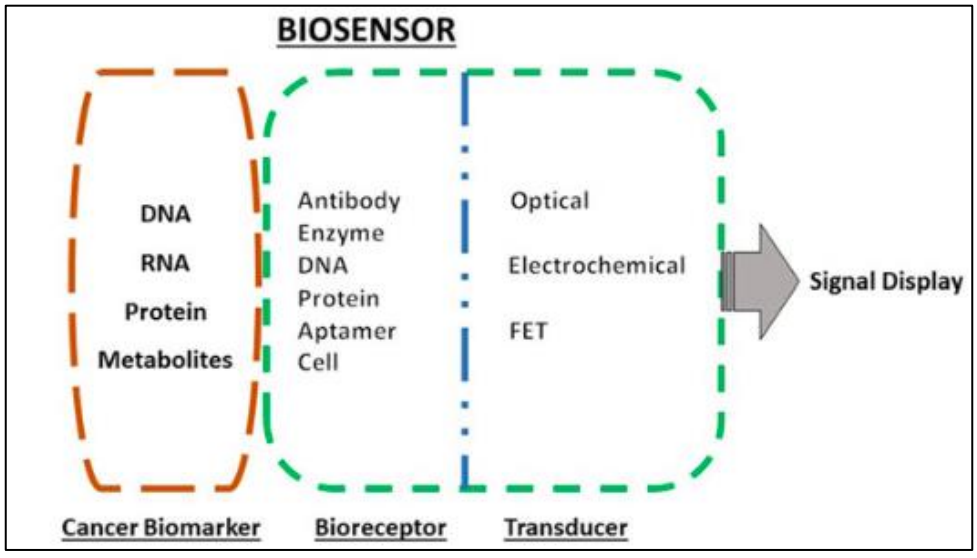

Figure I.3 : Schematic diagram of cancer biomarker detection by a biosensor [21].

I.5 Characteristics of biosensors

The design of biosensors must adhere to specific characteristics or parameters, essential for their performance and practical utility in various applications.

- *Selectivity*: The paramount consideration in biosensor design is selectivity, achieved through the careful selection of a bioreceptor. A proficient bioreceptor can effectively target analyte molecules amidst a mixture of samples containing other contaminants [22].
- *Sensitivity*: The limit of detection refers to the minimum amount of analyte that can be correctly detected/identified in a minimum number of steps and in low concentrations (in the range of ng/mL or fg/mL), thus confirming the presence of analyte traces in the sample [18].
- *Stability*: In biosensor applications demanding continuous monitoring, stability emerges as a crucial characteristic. Stability reflects the susceptibility to environmental disturbances both within and outside the biosensing device. Factors influencing stability include the bio receptor's affinity (the degree of analyte binding) and the degradation of the bio receptor over time [18].
- *Linearity*: enhances the precision of measured results. A great degree of linearity, represented by a straight line, corresponds to increased accuracy in detecting substrate concentrations [18].
- *Response time*: The time is taken for obtaining 95% of the results [18].
- *Reproducibility*: stands out as the paramount characteristic in biosensors. Consistency in results is crucial, implying that the biosensor should yield the same outcomes under identical conditions. This consistency, termed precision, ensures a uniform output signal when measuring the same sample multiple times. Achieving a mean value close to the actual value with precision and accuracy is essential for the effective application of a sensor [22].

I.6 Classification of biosensors

Biosensor classification is a multifaceted and interdisciplinary domain, encompassing diverse criteria. **Figure I.4** illustrates the overarching classification scheme outlining various criteria for categorizing biosensors.

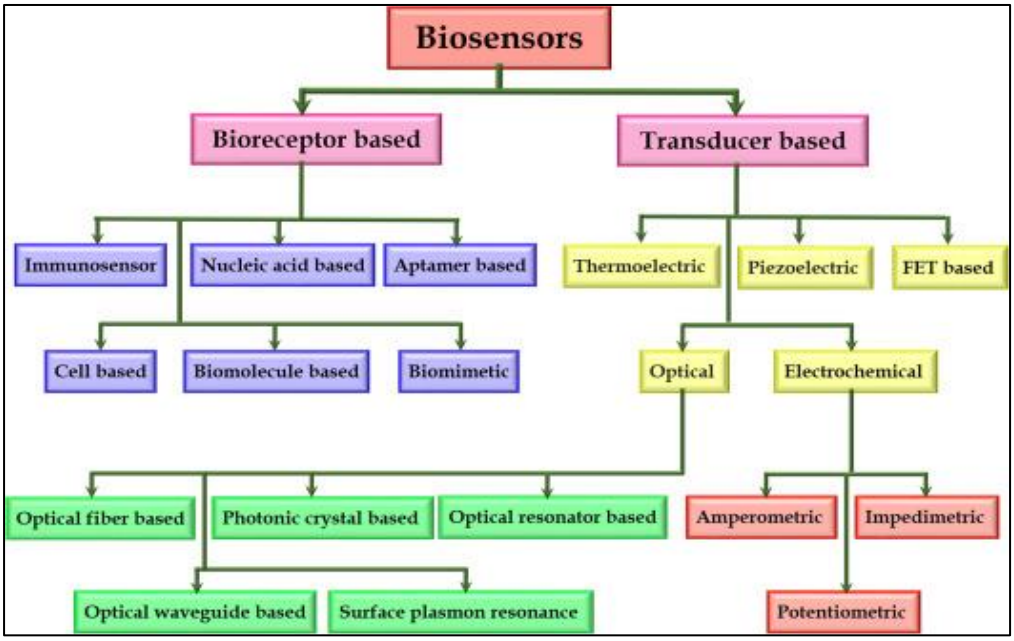

Figure I.4 : Classification of biosensors based on various bioreceptors and transducers used [23].

I.6.1 Classification based on biological receptors

- **Enzyme based biosensors:** Enzymes, large protein molecules in biosensors, trigger chemical reactions in living organisms. Their effectiveness is influenced by specific molecules like inhibitors and activators, which respectively decrease or increase enzyme activity. Enzymes act on molecules known as substrates in their active region, transforming them into products. The enzyme then moves to another region, and this process is sequential if multiple substrates are present. The high selectivity of enzymes makes them widely favored for biosensors [24-25].
- **DNA based biosensors:** Nucleic acid, the vital repository of genetic information, consists of complex protein molecules forming double strands with covalent bonds. These strands, composed of four nitrogenous bases, namely thymine, guanine, adenine, and cytosine, transfer an organism's genetics, stored within DNA. Nucleic acid biosensors, working on DNA strands, identify small segments, measure antigen bond strength, and gauge the intensity of recognition for foreign nucleic acids within

the body. These sensors, introduced in 1953, play a crucial role in stimulating immune cells to produce antibodies, protecting the body against germs or viruses [26-27].

– **Antibody based biosensors:** Y-shaped proteins created in the lymphatic system, actively encapsulate and break down foreign bodies. They analyze the genetic codes of these bodies for easy identification upon re-entry. The Y antibody structure comprises immunoglobulin (Ig), with two connected chains – polypeptide light chains and heavy chains- linked by disulfide bonds. Antibodies, classified into types such as IgD, IgE, IgG, IgA, and IgM, serve as lymphatic sensors or immunosensors for allergens utilizing this biological material [28-29].

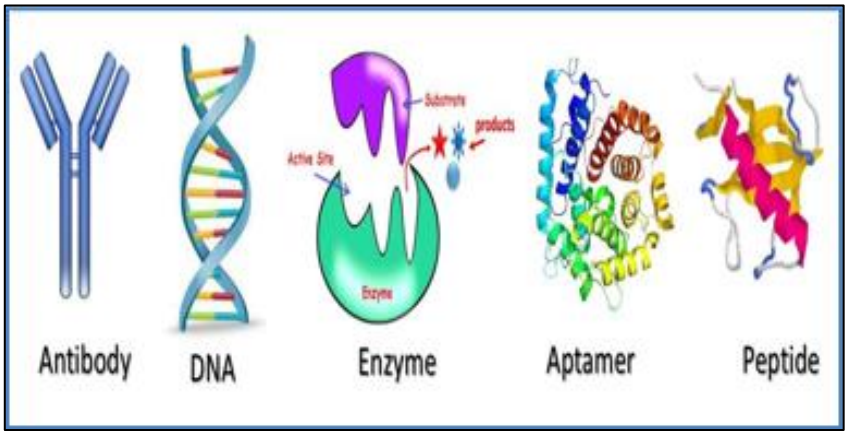

Figure I.5 : Bioreceptors types [30].

I.6.2 Biosensors based on transduction element

A transducer-based biosensor relies on the physical or chemical signals resulting from the interaction between the analyte and the bioreceptor to generate a measurable output. Here's a brief overview of these biosensor types and their working mechanisms, including explanations of some subclasses within each category.

– **Electrochemical biosensors:** Biosensors that utilize the electrochemical properties of the analyte or transducers for detection are referred to as electrochemical biosensors. These biosensors exhibit high selectivity and sensitivity. In electrochemical sensors, the bioreceptor and analyte trigger electrochemical reactions on the transducer's surface, generating detectable signals in the form of voltage, current, impedance, and capacitance [31]. Electrochemical biosensors are further classified based on transduction principles, including potentiometric, impedimetric, voltammetric, amperometric, and conductometric biosensors [32].

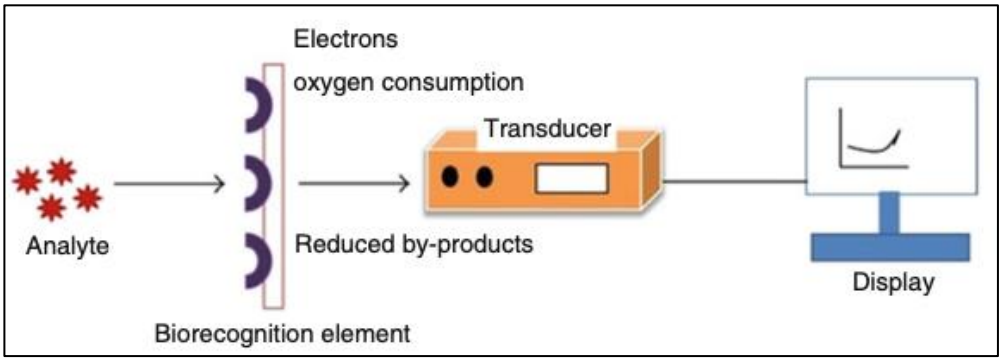

Figure I.6 : Schematic diagram of electrochemical biosensor [33].

- **Mass based biosensors:** Piezoelectric sensors operate based on sound vibrations, measuring the frequency change of a crystal resonator with mass per unit area. They generate an electrical signal when subjected to mechanical force. In lung cancer diagnosis, piezoelectric biosensors utilize elements like the p53 gene, nucleic acids, antibodies, and biomolecules. These sensors offer flexibility in design, can be tailored to desired sizes and shapes, and exhibit temperature sensitivity. Quartz, favored for its chemical, electrical, and mechanical properties, is a commonly used crystal for piezometric sensors. For lung cancer detection, these sensors undergo mutations at various points, and the resulting frequency changes are analyzed. They are effective in diagnosing viruses, proteins, ligands, and nucleic acids, being easy to develop, cost-effective, and highly sensitive [34].
- **Optical biosensor:** optical biosensors quantify changes in the optical properties of substances. Common types include surface Plasmon resonance (SPR), optical fiber, fluorescent, interference spectroscopy, and Raman scattering. In cancer cell detection, optical sensors rely on reflectivity changes. Biosensors respond to alterations in the refractive index near the sensor surface, detecting changes in reflectivity. Optical biosensors utilize CEA, TP53, and EGFR biomarkers for lung cancer detection, offering advantages like safety, flexibility, and compact size [35].
- **Thermal biosensors:** Thermal biosensors exploit the inherent property of biological reactions to either absorb or produce heat, thereby causing changes in the temperature of the reaction medium. Enzyme molecules, immobilized on a substrate, are integrated with temperature sensors. The heat generated or absorbed during enzymatic reactions with the analyte is quantified and correlated with the concentration of the analyte. These biosensors are widely utilized for detecting pesticides and pathogenic bacteria due to their sensitivity and specificity [36].

I.7 Applications of biosensor

Biosensors are crucial in disease detection, drug target identification, drug discovery, environmental monitoring, food safety, and the identification of defense-related toxic agents. They contribute to enhancing quality of life, stability, and sensitivity [37].

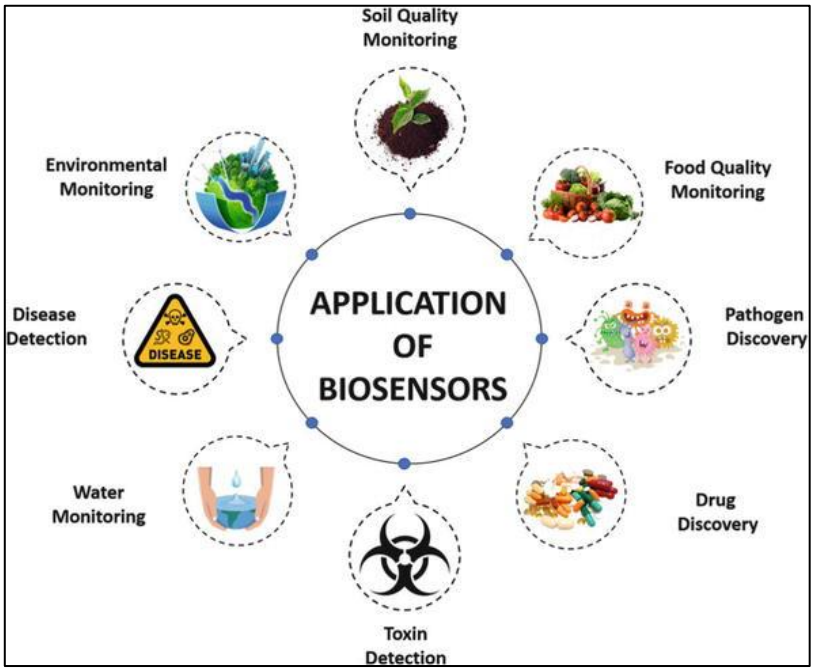

Figure I.7 : Applications of biosensors [38].

Medical:

- **Covid-19 detection:** Biosensors play a vital role in detecting respiratory viruses, such as Covid-19, using a simple saliva sample. Results are obtained within minutes, indicating infection status and antibody levels. These biosensors, particularly FET-based devices using materials like graphene, offer quick and sensitive detections, crucial in the face of emerging viruses. Their accuracy and speed make them valuable tools for doctors in diagnosing and planning effective treatments [39].
- **Cancer detection:** Cancer, a leading cause of global mortality with increasing incidence, claims millions of lives annually. Early diagnosis and treatment significantly impact survival rates, offering the potential to avoid 30 to 40% of cancer-related deaths. Biosensors, employing surface Plasmon resonance (SPR) principles, play a crucial role in early cancer detection. These devices convert biological reactions into electrical signals, allowing the identification of tumor cells as analytes. By detecting specific proteins released or expressed by tumor

cells, biosensors contribute to determining the nature of the tumor, aiding in the early identification of malignancy [39].

Environmental pollution: environmental pollution levels, detrimental to human health, are gauged using sensors. An example includes assessing the percentage of toxins in sewage water through the oxidation of organic pollutants like organophosphates, commonly used insecticides. This study aims to unveil the environmental impact of these substances. Bioreceptors such as aptamers, antibodies, DNA, and enzymes are preferred components in environmental monitoring [40-41].

Safety food: Nanosensors placed inside food packages play a vital role in ensuring food safety. They monitor the internal and external conditions of the food product, detecting changes caused by microbial or bacterial activity. The nanosensors exhibit color changes, accurately signaling even minimal microbe concentrations. Immunosensors are particularly effective for this purpose [42-43].

I.8 Challenges of traditional biosensors

Despite advancements in biosensor development across various fields, the commercial availability of these biosensors remains limited, posing a significant challenge. The difficulty lies in obtaining sensors with precise accuracy, specific sensitivity, and consistent repeatability to ensure reliable results for each application. In sectors like agriculture, food industry, and chemical pollutant monitoring, additional challenges include ensuring resistance to water and open-air exposure to maintain efficiency during repetitive use. Currently, the polymerase chain reaction (PCR) technique used for diagnosing diseases like Coronavirus is time-consuming, requires expensive and complex equipment, and demands highly skilled personnel. Furthermore, issues related to low sensitivity may result in false-negative or false-positive results [44-45].

I.9 Microwave biosensors

Microwaves are high-frequency, non-ionizing electromagnetic radiation used in daily devices like mobile phones [46]. Presently, low-power microwave technology is readily available, affordable, and poses no health risks. Material response to electromagnetic waves is influenced by complex permittivity, a key material property [47].

Among this diverse range of sensor types, microwave sensors stand out for material characterization due to their ability to easily penetrate the measured material using

electromagnetic (EM) waves. This distinctive feature, coupled with the advantages of label-free detection, seamless integration with measurement equipment, and the capability to characterize and monitor changes in material parameters, has led to the widespread adoption of microwave sensors in various applications, including those in the biological domain [48]. Broadly, two categories of microwave sensors exist based on their frequency range of operation: broadband and resonant sensors [49]. The choice between these types depends on the specific requirements, with broadband sensors providing comprehensive spectral information but at the cost of broadband measurement, while resonant sensors offer high sensitivity at discrete frequency point(s) with reduced equipment demands.

I.9.1 S-Parameters

Scattering parameters, or S-parameters, are frequency-dependent metrics used to characterize the transmission and reflection properties of high-frequency circuits, components, devices, and systems. They are expressed as complex numbers representing magnitude (in decibels, dB) and phase angle (in degrees). S-parameters are dimensionless and follow a specific nomenclature based on the number of ports.

For a one-port device (two connections, two poles), a single S-parameter (S_{11}) describes the reflection at the port. A two-port device (quadrupole) is characterized by four S-parameters: S_{11}, S_{21}, S_{12}, and S_{22}, which are used to describe most circuits and RF modules [50].

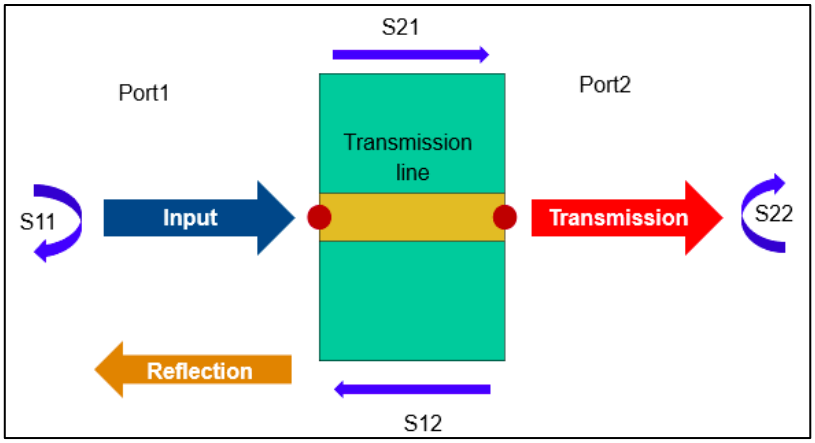

Figure I.8: Four S-parameters of a quadrupole [51].

The parameters S_{11} and S_{22} represent reflection coefficients, while S_{21} and S_{12} represent transmission coefficients. S_{11} indicates how well the input impedance matches the measuring line's impedance, typically 50 ohms or 75 ohms, with a low S_{11} value signifying low return loss. S_{21} pertains to transmission, indicating the insertion loss or gain caused by the device.

For passive, bidirectional components, S_{12} is equivalent to S_{21}. S_{22} relates to how well the output matches the impedance of the measurement system.

MIMO systems: In the case of a MIMO biosensor, scattering parameters provide more information than just the reflection coefficients. For a two-element MIMO system:

- S_{11} is the reflection coefficient of biosensor element 1.
- S_{22} is the reflection coefficient of biosensor element 2.
- S_{21} represents the ratio of power seen at the port of biosensor element 2 when biosensor element 1 is excited.
- S_{12} represents the ratio of power seen at the port of biosensor element 1 when biosensor element 2 is excited.

These scattering parameters (S_{21} and S_{12}) represent the isolation between ports in a two-element MIMO system. Effective MIMO systems require diversity, which necessitates a very low isolation coefficient between the antenna elements for efficient performance [52].

In microwave biosensors, S-parameters provide valuable information about the interaction between the sensor and the biological sample being analyzed. They enable the measurement and analysis of the electromagnetic response of the system, which is influenced by the properties of the sample, such as its dielectric properties, composition, and structural changes. This information is crucial for understanding and monitoring biological processes, making S-parameters essential tools in the development and application of microwave biosensors.

I.10 Metamaterial

Metamaterials are specially engineered materials comprising various structures and substances, featuring unique properties influenced by factors like orientation, dimension, shape, and base material. These distinct properties encompass negative electrical permittivity, magnetic permeability, and refractive index. Metamaterials have garnered attention for their capability to interact with electromagnetic waves, even when smaller than the wavelength. In recent years, they have played a crucial role in sensing technology, particularly in electromagnetic sensors. These sensors leverage alterations in the electromagnetic field during interaction with the tested material, causing shifts in resonance frequency and changes in response signal amplitude at a designated port [53].

In 1967, V.G. Veselago, associated with the Moscow institute of Physics and Technology, proposed the theoretical model of a medium now recognized as a metamaterial. However, physical experimentation was delayed for 33years after the paper’s publication due to the

unavailability of materials and insufficient computing power. It wasn't until the 2000s that both materials and computing power became accessible, enabling the artificial production of the required structures [54].

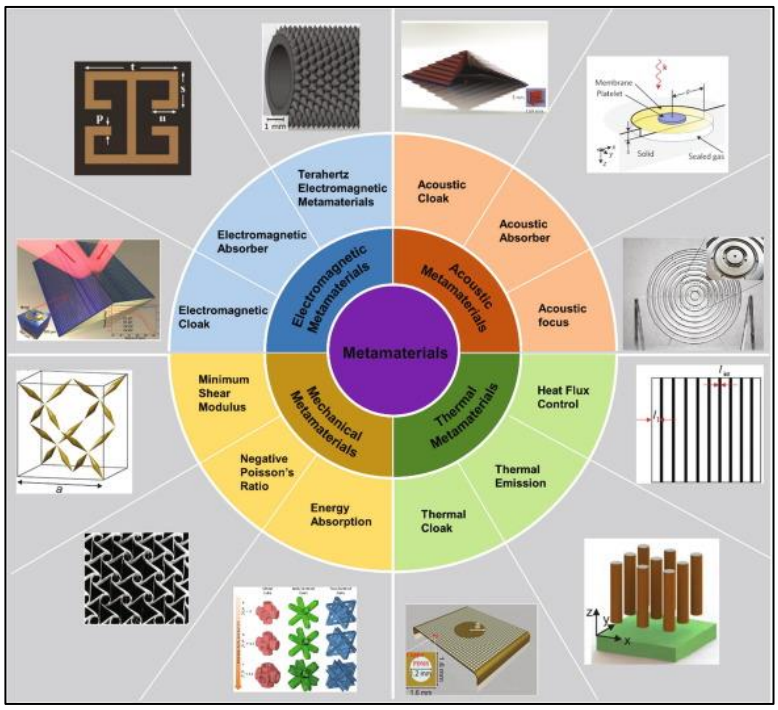

Figure I.9 : Additive manufacturing of metamaterials [55].

I.10.1 The impact of metamaterials in biosensing applications

Metamaterials, with their unique properties, are promising for biosensing applications, particularly in microwave biosensors. They offer efficient electromagnetic radiation absorption, miniaturization, adaptability, and enhanced effectiveness compared to traditional methods. Metamaterial-based biosensors interact with target biological molecules, causing changes in light properties for detection. These biosensors provide sensitivity, selectivity, rapid response, low detection limits, and compatibility with various samples. Metamaterials can also create filters to enhance specificity by selectively detecting specific biological molecules based on resonant frequencies in the microwave range [56].

I.10.2 Split ring resonators

Another type of metamaterial structure relies on sub-wavelength resonators, primarily utilizing split ring resonators (SRR). First introduced by Pendry, this resonant approach offers compact structures with high design flexibility, making them conductive to miniaturization. Various resonant particle approaches based on SRR have been developed and applied in numerous microwave applications. Their versatility allows coupling in different ways, such as with coplanar, stripline, and microstrip designs, adding a planarity feature. Depending on the

resonator and coupling types, different propagation characteristics can be tailored to meet specific requirements. It's crucial to note that this resonant approach employs resonators as loading elements [57].

SRRs consist of a metallic loop with one or multiple small gaps and can assume various shapes like circular, square, or hexagonal. Circular and rectangular SRRs are the most commonly utilized, with rectangular SRRs offering distinct advantages. They facilitate superior miniaturization, denser packing, and more robust magnetic coupling compared to circular resonators [58].

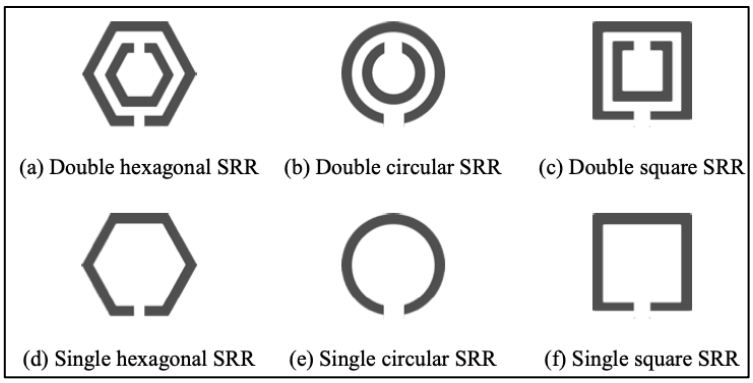

Figure I.10 : Split ring resonator designs [56].

I.10.3 Metamaterial Antenna

Metamaterials antennas utilize metamaterials to improve the efficiency of electrically small or miniaturized antenna systems. By leveraging metamaterials, these antennas can significantly reduce their size while simultaneously enhancing attributes like bandwidth, gain, and multi-band frequency functionality. The integration of metamaterials into the antenna design allows them to achieve superior performance compared to conventional antennas. The antenna depicted in **Figure I.11** is constructed based on SRR technology [59].

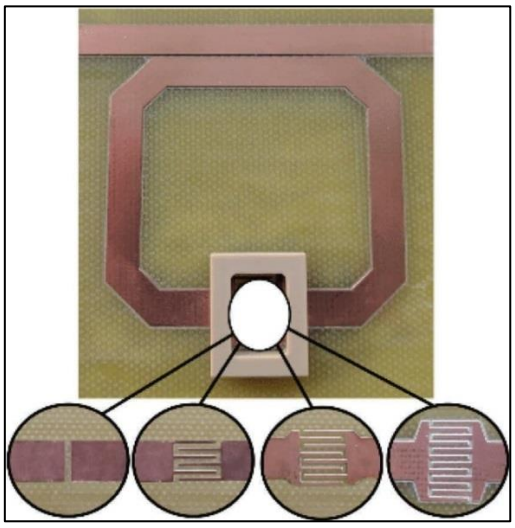

Figure I.11 : Antenna based on split-ring resonator [59].

I.11 MIMO sensors

In wireless communication, antennas serve as key devices facilitating communication between transmitters and receivers using radio waves. They can be designed for uniform transmission in all directions or with a specific directional preference. Two main types of antennas, SISO (single input single output) and MIMO, are commonly used for various applications. SISO antennas, though easy to design, face challenges like multipath effects and fading. To address these, smart antenna technology is utilized, leading to the development of MIMO antennas for enhanced performance and overcoming limitations [60].

Originally, MIMO denoted the use of multiple antennas on both the transmitter and receiver. However, in current usage, MIMO commonly describes a practical technique for transmitting and receiving multiple data signals over a signal radio channel, utilizing multipath propagation. MIMO operations encompass three primary categories: precoding, beamforming, and decoding [61]. MIMO technology, a revolutionary advancement in wireless communication, was developed in the late 1990s and early 2000s by various companies, including Airgo Networks, later acquired by Qualcomm in 2006 [59].

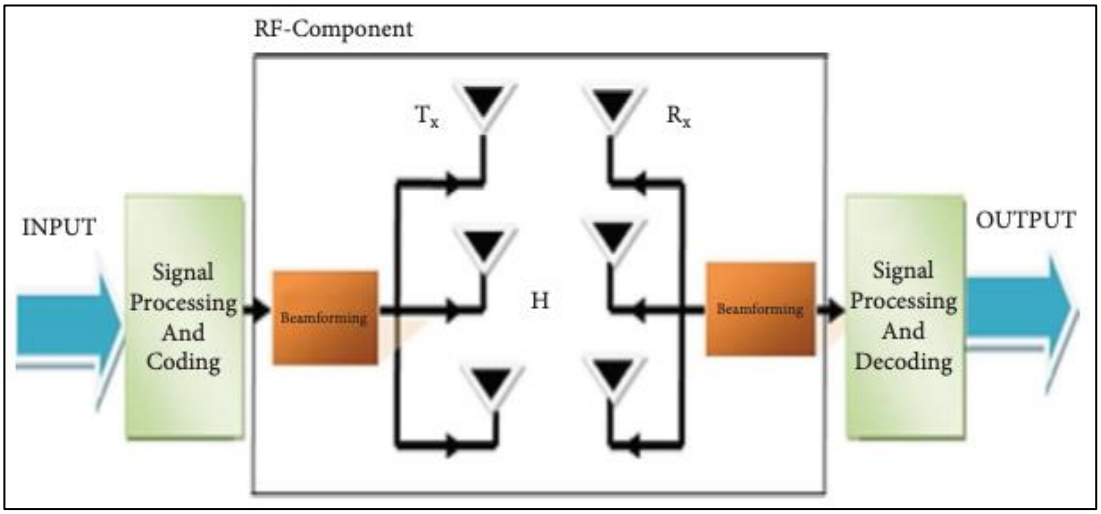

Figure I.12 : General model of the MIMO system [59].

In MIMO designs, two or more radiating elements are fed separately using coplanar or strip line feeding techniques to transmit and receive data. However, port coupling is a major concern in MIMO design, as it degrades antenna performance. One effective approach to achieve good isolation is to use a metamaterial-based MIMO design. For instance, a suspended meta-surface made up of periodic square SRRs can be placed above the antenna array. These SRRs, composed of inductive lines and capacitive gaps, facilitate both magnetic and electric coupling, enhancing isolation and reducing mutual coupling. Such designs ensure better decoupling, improving the overall performance of MIMO antennas in high-speed communication technologies.

I.11.1 MIMO antenna

MIMO antennas have received much attention in the modern wireless communication system as it can use multi-paths to transmit or receive data, and hence increase the range and output performance. It is noted that the significant isolation between components of the same MIMO system is necessary so that elements of the MIMO antenna can work independently to transmit or receive signals simultaneously without deteriorating the antenna parameters. In order to ensure the quality of a MIMO antenna, in addition to S-parameters and radiation characteristics, certain diversity parameters are used. The MIMO antennas must satisfy the predefined values of the diversity parameters for practical applications.

I.11.2 Advantages of MIMO antennas in 5G applications

Advantages of MIMO antennas include [59]:

- Faster data transfer rates through simultaneous transmission and reception of multiple data streams over the same frequency band.
- Increased network capacity by allowing multiple users to transmit and receive data simultaneously.
- Mitigation of interference and signal fading for more reliable communication using multiple antennas.
- Higher spectral efficiency achieved by transmitting multiple data streams in the same frequency band.

I.12 Conclusion

In conclusion, biosensors play a crucial role in the early detection of lung damage levels, revolutionizing health diagnostics. Providing an essential understanding of biosensor fundamentals, historical contexts, and extensive applications, we establish the cornerstone for disease management. As we advance into the forefront of biosensing technologies, the integration of Metamaterials into MIMO sensor antennas emerges as a promising breakthrough.

Metamaterials profoundly impact MIMO antenna systems, enhancing their performance and capabilities. By harnessing Metamaterials, MIMO sensors can process multiple input signals concurrently, bolstering detection capabilities and amplifying sensitivity and precision in identifying lung damage levels. This synergy between Metamaterials and MIMO sensor technology heralds a new era of biosensing, where unprecedented levels of accuracy and efficiency become attainable.

REFERENCES

[1] Archived: WHO Timeline - COVID-19-April 2020. https://www.who.int/news/item/27-04-2020-who-timeline---covid-19 (accessed Mai 27, 2024).

[2] World Health Organization. (2023). The current COVID-19 situation: Algeria. https://www.who.int/countries/dza (accessed Mai 27, 2024).

[3] N. Poyiadji, G. Shahin, D. Noujaim, M. Stone, S. Patel, & B. Griffith, "*COVID-19–associated acute hemorrhagic necrotizing encephalopathy: CT and MRI features*," Radiology, 296(2), 246–248, 2020.

[4] L. Mao, H. Jin, M. Wang, et al, " *Neurologic manifestations of hospitalized patients with coronavirus disease 2019 in Wuhan, China,"* JAMA Neurol, 77(6), 683-690, 2020.

[5] D.J.H. Bian, S. Sabri, B.S Abdulkarim, "*Interactions between COVID-19 and Lung Cancer: Lessons Learned during the Pandemic*," Cancers, 14, 3598, 2022, https://doi.org/10.3390/ cancers14153598.

[6] A. Binte Anwar et al, " *Performance of a 5G MIMO Antenna for Detecting Damaged Lungs of Pneumonia Patients Related to Covid-19*," International Journal of Scientific & Engineering Research, vol. 12, issue 7, ISSN 2229-5518, July 2021.

[7] M.J. Cha, J.J. Solomon, J.E. Lee, H. Choi, K.J. Chae, K.S. Lee, & D.A. Lynch, " *Chronic lung injury after COVID-19 pneumonia: Clinical, radiologic, and histopathologic perspectives*". *Radiology, 310*(1), 2024. https://doi.org/10.1148/radiol.231643

[8] A.B. de González, S. Darby, " *Risk of cancer from diagnostic X-rays: estimates for the UK and 14 other countries*, " Lancet 363, 345–351, 2004.

[9] L. Wang, " *Screening and Biosensor-Based Approaches for Lung Cancer Detection.* " Sensors (Basel), 17(10), 2420, 2017, https://doi.org/10.3390/s17102420 .

[10] M. Pal, T. Muinao, A. Parihar, D.K. Roy, H.P.D. Boruah, N. Mahindroo, & R. Khan, "*Biosensors based detection of novel biomarkers associated with COVID-19: Current progress and future promise*," Elsevier - PMC COVID-19 Collection, 2022. https://doi.org/10.1016/j.biosx.2022.100281

[11] BD. Malhotra et al, "*Recent trends in biosensors*," Current Applied Physics, 5(2), 92-7, 2005.

[12] Tran Minh Canh, "*Biosensors*," Ecole Nationale Supérieure des Mines Saint-Etienne, France,1993.

[13] P. Tetyana, P. Morgan Shumbula & Z. Njengele-Tetyana, "*Biosensors: Design, Development and Applications. Nanopores*, " Intech Open, 2021,

DOI: 10.5772/intechopen.97576.

[14] J. Castillo et al. "*Biosensors for life quality Design, development and applications*," Sensors and Actuators B, 102, 179-194, 2004, DOI: 10.1016/j.snb.2004.04.084.

[15] N. Bhalla, P. Jolly, N. Formisano, P. Estrela, "*Essays in Biochemistry*," 60, 1-8, 2016, DOI: 10.1042/EBC20150001.

[16] BM. Paddle, "*Biosensors for chemical and biological agents of defence interest*," Biosensors & Bioelectronics, 11(11), 1079-1113, 1996, DOI: 0956-5663/961515.00.

[17] JE. Pearson, A. Gill, P. Vadgama, "*Analytical aspects of biosensors*," Annals of Clinical Biochemistry, 37, 119-145, 2000.

[18] DR. Thevenot, K. Toth, RA. Durst, GS. Wilson, "*Electrochemical biosensors: recommended definitions and classification*," Biosensors and Bioelectronics, 16, 121-131, 2001, DOI.org/10.1016/S0956-5663(01)00115-4.

[19] D. Grieshaber, R. MacKenzie, J. Vörös, E. Reimhult, "*Electrochemical Biosensors - Sensor Principles and Architectures*," Sensors, 8(3), 1400-1458, 2008.

[20] V. Perumal, U. Hashim, "*Advances in biosensors: Principle, architecture and applications*," Journal of Applied Biomedicine, 12(1), 1-15, 2014.

[21] R. Malviya, S. Sundram, (eds.). "*Targeted Cancer Therapy in Biomedical Engineering*," Biological and Medical Physics, Biomedical Engineering, 2023, https://doi.org/10.1007/978-981-19-9786-0_12

[22] P.P.M.S. Rahman, M. Joseph, L.V. Nair, T. Hanas, *" Emerging Materials for Biosensor Applications in Healthcare*, " (eds) Emerging Materials. Springer, Singapore, 2022, https://doi.org/10.1007/978-981-19-1312-9_7

[23] A. Sharma, A. Agrawal, S. Kumar, K.K. Awasthi, K. Awasthi & A. Awasthi," *Zinc oxide nanostructures–based biosensors,* " In K. Awasthi (Ed.), Metal Oxides, Nanostructured Zinc Oxide (pp. 655-695). Elsevier, 2021, https://doi.org/10.1016/B978-0-12-818900-9.00002-4

[24] D. Diamond, Chemical and Biological Sensors (Vol. 45). Wiley, New York, 1998.

[25] W.-W. Zhao, J.-J. Xu, H.-Y," *Photoelectrochemical enzymatic biosensors*," Biosensors and Bioelectronics, 92, 294-304, 2017.

[26] A. Tan, C. Lim, S. Zou, Q. Ma, Z. Gao," *Electrochemical nucleic acid biosensors: from fabrication to application*," Analytical Methods, 8, 5169-5189, 2016

[27] Y. Du, S. Dong, " *Nucleic acid biosensors: recent advances and perspectives*. " Analytical Chemistry, 89, 189-215, 2017.

[28] P.K. Ferrigno, " *Non-antibody protein-based biosensors,* " Essays in Biochemistry, 60, 19-25, 2016.

[29] E.A. Padlan, " *Anatomy of the antibody molecule,* " Molecular Immunology, 31, 169-217, 1994.

[30] H.N. Noori, A.F. Abdulameer, "*A Review of Biosensors; Definition, Classification, Properties, and Applications,*" Iraqi Journal of Science, 64(11), 5665-5690, 2023, https://doi.org/10.24996/ijs.2023.64.11.18

[31] D. Grieshaber, R. MacKenzie, J. Vörös, E. Reimhult, "*Electrochemical biosensors—sensor principles and architectures,*" Sensors, 8(3), 1400–1458, 2008, https://doi.org/10.3390/s80314000

[32] A. Chaubey, B.D. Malhotra, "*Mediated biosensors,*" Biosens. Bioelectron. 17(6–7), 441–456, 2002, https://doi.org/10.1016/S0956-5663(01)00313-X

[33] S. Bag, D. Mandal, "*Overview of Biosensors and Its Application in Health Care,*" In: Dutta, G., Biswas, A. (eds) Next Generation Smart Nano-Bio-Devices. Smart Innovation, Systems and Technologies, vol 322. Springer, Singapore, 2023, https://doi.org/10.1007/978-981-19-7107-5_3

[34] B. Buszewski, M. Kesy, T. Ligor, A. Amann, "*Human exhaled air analytics biomarkers of diseases,*" Biomedical Chromatography, 21, 553-66, 2007, DOI: 10.1002/bmc.835

[35] F. Usman, J.O. Dennis, A.I. Aljameel, M.K.M. Ali, O. Aldaghri, K.H. Ibnaouf & al, " *Plasmonic Biosensors for the Detection of Lung Cancer Biomarkers: A Review.* " Chemosensors, 9, 326, 2021, https://doi.org/10.3390/chemosensors9110326

[36] R. Syam, KJ. Davis, M. Pratheesh, R. Anoopraj, BS. Joseph, "*Biosensors: A Novel Approach for Pathogen Detection,*" VETSCAN, 7(1), 14-18, 2012.

[37] P. Arora, A. Sindhu, N. Dilbaghi, A. Chaudhury, "*Biosensors as innovative tools for the detection of food borne pathogens*." Biosens Bioelectron, 28(1), 1-12, 2011.

[38] Singh S, Kumar V, Dhanjal DS, Datta S, Prasad R, Singh J. " *Biological Biosensors for Monitoring and Diagnosis,* " Microbial Biotechnology: Basic Research and Applications. 2020 Jul 8:317–35. DOI: 10.1007/978-981-15-2817-0_14.

[39] S. Sawant, S. Shiralkar, "*All about Biosensors-A Review,*" Journal of Engineering and Technology Management, April 2022. Available: https://www.researchgate.net/publication/360110407.

[40] M. Gavrilescu, K. Demnerová, J. Aamand, S. Agathos, F. Fava, "*Emerging pollutants in the environment: present and future challenges in biomonitoring, ecological risks and bioremediation,*" New biotechnology, 32, 147-156, 2015.

[41] V.K. Nigam, P. Shukla, "*Enzyme based biosensors for detection of environmental pollutants-a review,*" Journal of microbiology and biotechnology, 25, 1773-1781, 2015.

[42] B. Van Dorst, J. Mehta, K. Bekaert, E. Rouah-Martin, W. De Coen, P. Dubruel, & al, "*Recent advances in recognition elements of food and environmental biosensors: A review*," Biosensors and Bioelectronics, 26, 1178-1194, 2010.

[43] T.K. Sharma, R. Ramanathan, R. Rakwal, G.K. Agrawal, V. Bansal, "*Moving forward in plant food safety and security through NanoBioSensors: Adopt or adapt biomedical technologies?*" Proteomics, 15, 1680-1692, 2015.

[44] C.I. Justino, A.C. Duarte, T.A. Rocha-Santos, "*Recent progress in biosensors for environmental monitoring: A review*," Sensors, 17, 2918, 2017.

[45] J. Li, N. Wu, "Biosensors based on nanomaterials and nanodevices," CRC Press, 2013.

[46] L. Wang, (Ed.) "*Electromagnetic Waves and Antennas for Biomedical Applications*," Healthcare technologies series, Institution of Engineering and Technology, Stevenage, UK, 2022, ISBN 978-1-83953-167-5.

[47] M. Lazebnik, L. McCartney, D. Popovic, C.B. Watkins, M.J. Lindstrom, J. Harter & al, "*A Large-Scale Study of the Ultrawideband Microwave Dielectric Properties of Normal Breast Tissue Obtained from Reduction Surgeries*," Phys. Med. Biol., 52, 2637–2656, 2007.

[48] I. Piekarz, J. Sorocki, S. Gorska, H. Bartsch, A. Rydosz, R. Smolarz & al, "*High sensitivity and selectivity microwave biosensor using biofunctionalized differential resonant array implemented in LTCC for Escherichia coli detection*," Measurement, 208, 112473, 2023.

[49] L.F. Chen, C.K. Ong, C.P. Neo, V.V. Vardan, V.K. Vardan, "*Microwave Electronics: Measurement and Material Characterization*," Chi Chester, England: John Wiley and Sons, 2004.

[50] B. Eugen Born, " *Simulation of a double ridge horn and a log-periodic dipole antenna for EMC measurement* (Master's thesis) ", University of West Bohemia, 2018.

[51] "Scattering Parameters or S-Parameters," [Online]. Available : https://www.mathworks.com/help/rfpcb/gs/scatterring-parameters-or-s-parameters.html

[52] C.C. Arnold, " *Design, Fabrication, and Measurement of a Multiple-Input Multiple-Output (MIMO) Antenna for Mobile Communication* ". Graduate Theses and Dissertations Retrieved from https://scholarworks.uark.edu/etd/1194

[53] T. Chen, S. Li, H. Sun, "*Metamaterials Application in Sensing*," Sensors, 12(3), 2742-2765, 2012, DOI: 10.3390/s120302742.

[54] V.I. Slyusar, "*Metamaterials on antenna solutions*," In International Conference on Antenna Theory and Techniques, pp. 19-24, 2009.

[55] J. Fan, L. Zhang, S. Wei, Z. Zhang, S.-K. Choi, B. Song, Y. Shi, "*A review of additive manufacturing of metamaterials and developing trends*," Materials Today, 50, 303-328, 2021.

[56] N.M.N. Alrayes, "*Metamaterial-Based Sensor Design Using Split Ring Resonator and Hilbert Fractal for Biomedical Application*," Electrical Engineering Thesis, United Arab Emirates University, Apr. 2019.

[57] M.P. Vargas, "*Planar Metamaterial Based Microwave Sensor Arrays for Biomedical Analysis and Treatment*." Doctoral Thesis accepted by Technische Universität Darmstadt, Darmstadt, Germany. Springer International Publishing Switzerland, 2014, DOI: 10.1007/978-3-319-06041-5.

[58] A. Vallecchi, E. Shamonina, C.J. Stevens, "*Analytical model of the fundamental mode of 3D square split ring resonators.*" Journal of Applied Physics, 125(1), 014901, 2019.

[59] P. Tiwari, V. Gahlaut, M. Kaushik, P. Rani, A. Shastri, B. Singh, "*Advancing 5G Connectivity: A Comprehensive Review of MIMO Antennas for 5G Applications*." International Journal of Antennas and Propagation, Article ID 5906721, 19 pages, 2023, https://doi.org/10.1155/2023/5906721.

[60] L. Liu, S.W. Cheung, T.I. Yuk, "*Compact MIMO Antenna for Portable Devices in UWB Applications*, " IEEE Transactions on Antennas and Propagation, 61(8), August 2013.

[61] T.L. Marzetta," *Noncooperative cellular wireless with unlimited numbers of base station antennas*, " IEEE Transactions on Wireless Communications, 9(11), 3590–3600, 2010.

CHAPTER II

Artificial Neural Networks

II.1 Introduction

Over time, biosensors have evolved significantly, incorporating various technical improvements and advancements, achieving a high level of sophistication in diverse aspects. These sensors leverage powerful tools like artificial neural networks (ANN) to further enhance their capabilities. ANN plays a pivotal role in modeling and calibrating intricate biosensor signals, especially in non-linear scenarios. Serving as an adaptive filter, it enhances linearity, and maintains stability during training processes using pre-measured data. Once trained, ANN offers precise predictions in subsequent recall processes, solidifying biosensors as versatile and efficient analytical tools across various domains [1].

II.2 Definition and history

The Artificial Neural Network (ANN) has been a prominent topic in artificial intelligence since the 1980s. During this period, researchers abstracted the human brain's neural network for information processing, establishing a simplified model. ANNs simulate brain neural network processing by storing memory information through interconnected nodes, each representing a specific output function. The connections between nodes, known as weights, play a crucial role in signal transmission. Over the last ten years, significant progress has been made in ANN research, particularly in pattern recognition, intelligent robots, automatic control, prediction, estimation, biology, medicine, and economics [2]. This progress has addressed practical problems that traditional computers struggled with, showcasing the intelligence of ANNs.

The first wave of interest in these networks, also known as connectionist models or parallel distributed processing, emerged following the introduction of simplified neurons by McCulloch and Pitts in 1943 [3].

II.3 The biological neuron

Neurons are specialized cells essential for processing and interpreting information. At birth, humans possess around 100 billion neurons, with the majority concentrated within the brain [4].

Neurons consists of four main parts (**Figure II.1**):

- Dendrites: These are where other cells make synaptic contact; they receive signals.
- Cell body (Nucleus): it's the processing unit.
- Axon: Messages accumulated in the cell body pass through here; it's responsible for transmitting information.

- Synapses: These are points of connection through which the cell communicates with other cells; signals pass through them [5].

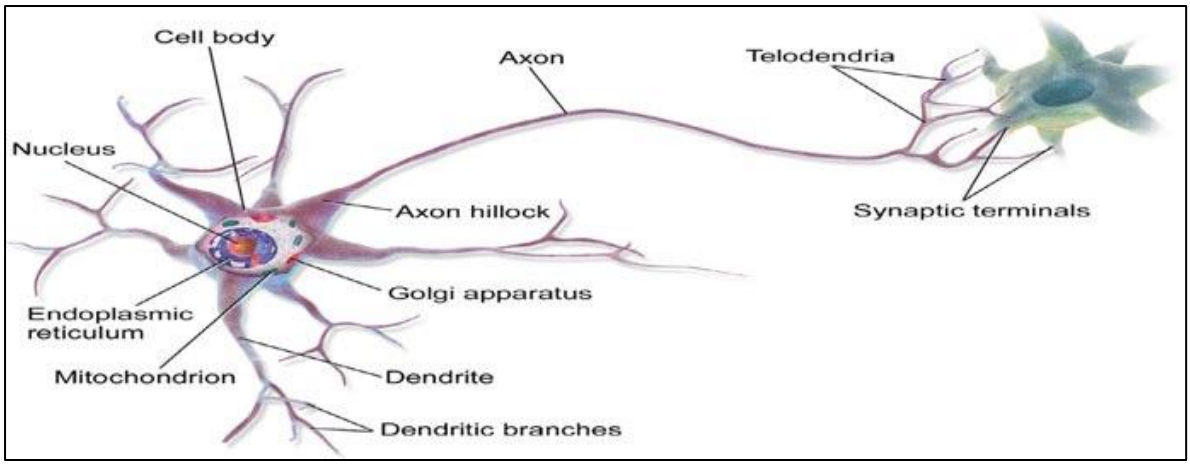

Figure II.1: A graphic representation of a biological neuron [6].

II.4 The perceptron model

When a new technique emerges in the field of computer science, engineers begin to construct an artificial neuron, which is a nonlinear algebraic function with bounded values. Each component of an artificial neuron corresponds to elements found in a biological neuron. An artificial neuron receives input variables from upstream neurons, with each input associated with a weight. Each elementary processor has a single output [7].

In 1943, McCulloch and Pitts proposed the first artificial neuron model, now called a perceptron, consisting of a binary threshold activation function (**Figure II.2**). This mathematical neuron calculates a weighted sum of its input signals and, if the sum is above a certain threshold, produces an output of "1", "0", or another positive number. Otherwise, the function returns "0" as the result, and this logic is also called the hardlim function [8].

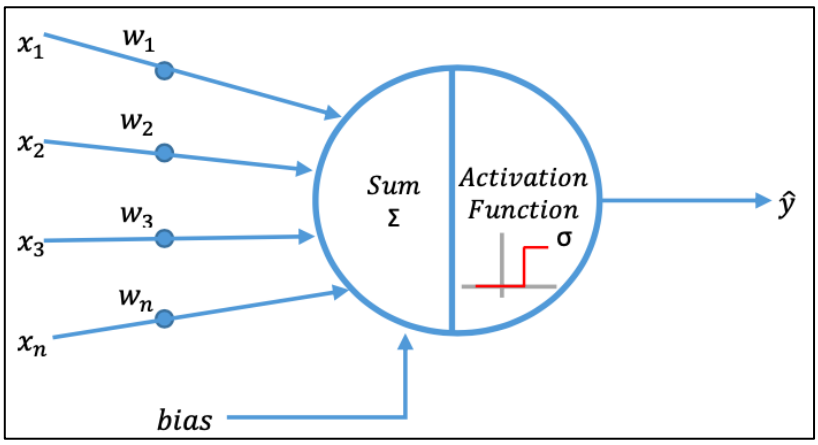

Figure II.2: Artificial neuron [8].

The perceptron applies a linear combination of its inputs, thereby obtaining a signal, to which an activation function is applied to obtain the output signal. Nonlinear functions are most commonly used to convey nonlinear behavior to the perceptron. The mathematical model of the perceptron is shown in Eq.II.1.

$$\hat{y} = \sigma(\sum_{i=1}^{n} x_i w_i + bias) \quad \textbf{(II.1)}$$

where $\hat{y}$ is the neuron output; σ is the activation function; x is the input vector of elements of n; w is the weight vector and $bias$ is the value that allows filtering of the activation function. The bias is somewhat similar to the constant b of the linear function $y = ax + b$ [8].

II.5 Component of artificial neural network

Components of ANN typically include [9]:

II.5.1 Input layer

This layer receives the initial data for the neural network. It does not perform any computations on the input values; rather, it directly passes them to the next layer.

II.5.2 Hidden layers

Situated between the input and output layers, the hidden layers act as the neural network's processing units. They are often referred to as the "black box". Each node in the input layer is connected to nodes in the hidden layers, and each hidden layer employs an activation function.

II.5.3 Output layer

Positioned at the end of the neural network, the output layers is responsible for making predictions. It receives the output from the hidden layers and processes it for evaluation. Like the hidden layers, the output layer also utilizes an activation function to provide probabilities for different outcomes.

II.5.4 Weights

These are parameters that the model adjusts during training. When inputs are passed through the neural network, weights assign importance to each input. Essentially, weights determine the impact of each input on the network's output.

II.5.5 Biases

Constant values added to the inputs of the next layer. Bias units always have a value of 1 and ensure that even if all input values are zero, there will still be activation in the neuron. While biases are not affected by the previous layer, they do have outgoing connections with their own weights.

II.6 Activation function

In the domain of artificial neural networks, the activation function serves as a crucial mathematical operation applied to the output signal of each artificial neuron. Stemming from its biological counterpart, the "activation potential", which denotes the stimulation threshold leading to neuron response, the activation function is typically non-linear [10]. This non-linearity is indispensable, as linear functions are limited to single-layer neural networks. Within a neuron, the activation function operates by computing the dot product between input signals and weight vectors while incorporating a bias term. Subsequently, the result undergoes transformation via the activation function, introducing non-linearity post-dot product computation. This non-linear property facilitates diverse internal state variations among objects of the same class [11]. However, the choice of an activation function is a crucial component of neural network. This function can significantly impact the network's performance. Therefore, selecting the appropriate type of activation function is essential in a neural network.

There can be many activation functions like:

II.6.1 Hardlim function

The Hardlim function, also known as the binary step function, is the first activation function proposed by McCulloch and Pitts, the fathers of artificial neurons. The function returns the binary output value "0" or "1", "0" if the signal value is less than "0", or "1" if the signal value is equal to or greater than "0". The formula is as follows:

$$f(x) = hardlim(x) = \begin{cases} 0 \; for \; x < 0 \\ 1 \; for \; x \geq 0 \end{cases} \qquad \textbf{(II.2)}$$

Today, Hardlim is rarely used because in most modern problems of interest, there is no linear relationship between input and output patterns [8].

II.6.2 Sigmoid function (Logistic function)

This function accepts real numbers as input and produces output values ranging between 0 and 1. As the input increases (becomes more positive), the output approaches 1, while for smaller inputs (more negative), the output tends towards 0 [9].

$$f(x) = \frac{1}{1+e^{-x}} \quad \textbf{(II.3)}$$

II.6.3 Tanh function (Tansig)

It's Hyperbolic Tangent function. this function closely resembles the sigmoid activation function, sharing the same S- shaped curve. It accepts any real number as input and produces output values within the range of -1 to 1. As the input increases (becomes more positive), the output approaches 1, while for smaller inputs (more negative), the output tends towards -1 [9]. Tanh is favored over the sigmoid function due to its gradients, which are not limited to a specific direction, and its characteristic of being zero-centered.

$$f(x) = \frac{e^{x}-e^{-x}}{e^{x}+e^{-x}} \quad \textbf{(II.4)}$$

II.6.4 ReLU function

The ReLU (Rectified Linear Unit) stands out as the most widely employed activation function globally. It finds application in nearly all convolutional neural networks and deep learning models. Essentially, it outputs the input value (x) if it's positive; otherwise, it yields 0 [9].

$$f(x) = \max(0, x) \quad \textbf{(II.5)}$$

II.6.5 Softmax function

The softmax function has been widely used in ANNs, especially in DNN architectures, and due to its properties, it is one of the few activation functions placed at the output layer. softmax has classifier properties because the function returns a number that can be interpreted as the probability of a particular class. The softmax formula is shown in Eq.II.6.

$$f(\vec{x}) = softmax(\vec{x}) = \frac{e^{x_i}}{\sum_{i=0}^{J} e^{x_j}} \quad \textbf{(II.6)}$$

Softmax ensures a probability distribution with the following properties: Each individual output ($\hat{y}_i$) of a set of observations ($\vec{x}$) satisfies the condition $0 \leq \hat{y}_i \leq 1$ and the sum of the outputs ($\sum_{i=0}^{J} \hat{y}_j$) is equal to "1", according to the requirements of probability. The Softmax activation function in the last layer of a text analysis ANN gives the probability of occurrence

of a word in a text string. In the same way, it calculates possible tags in sentiment analysis of tweets and gives the class probability for a specific image [8].

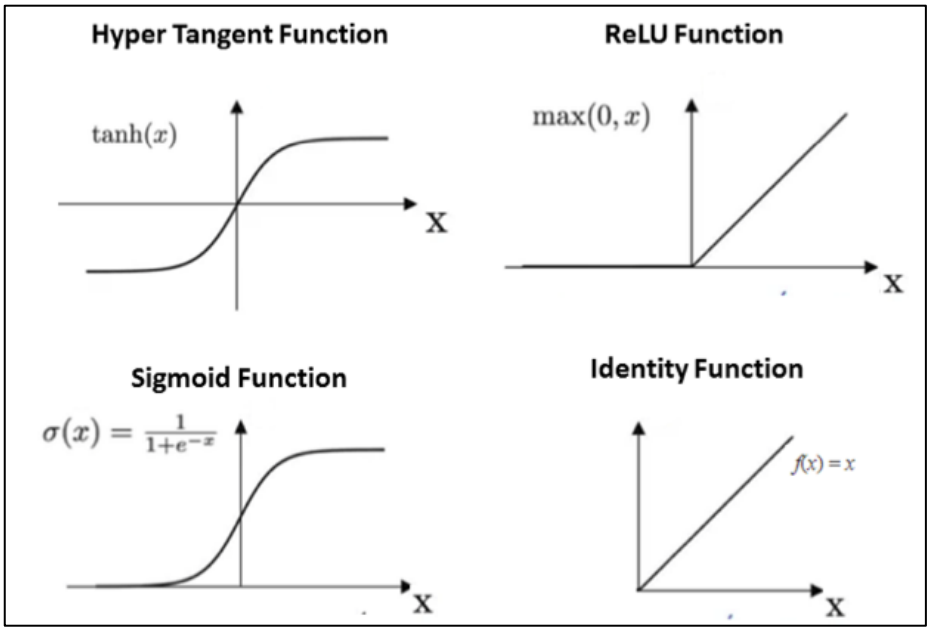

Figure II.3: Some activation function [12].

II.7 Architectures

An artificial neural network (ANN) functions as a parallel computing system, capable of addressing tasks beyond the capabilities of linear computing paradigms alone. It's categorized into two main types: feedforward networks and recurrent/feedback networks. This classification is depicted in **Figure II.4.** Our focus is on feedforward networks for their simplicity and effectiveness.

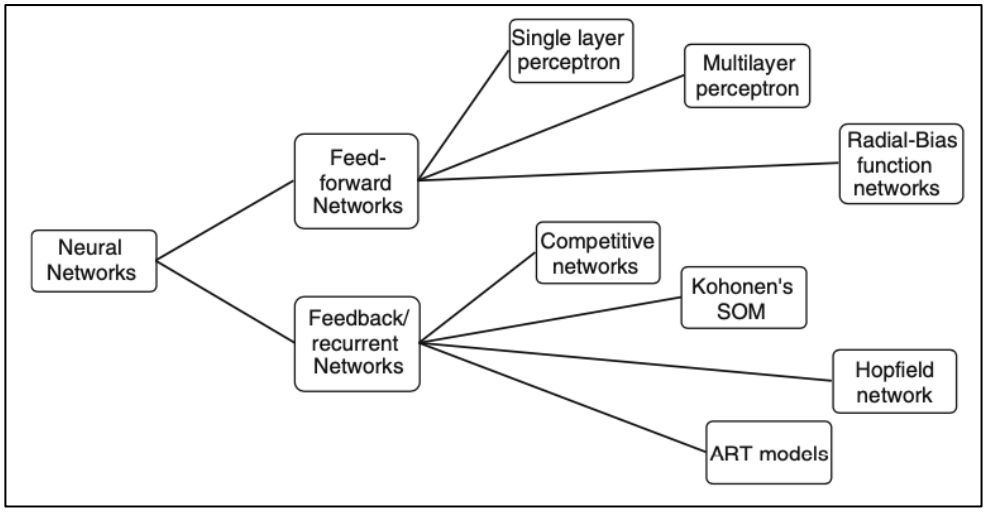

Figure II.4: Types of neural network architectures [13].

II.7.1 Single layer feedforward network

In its most basic form, a single-layer feedforward network consists of an input layer comprising neurons (source nodes) directly connected to an output layer of neurons (computation nodes), as depicted in **Figure II.5**. The input layer is not considered in the computation as it serves solely to relay input data to the output layer [14].

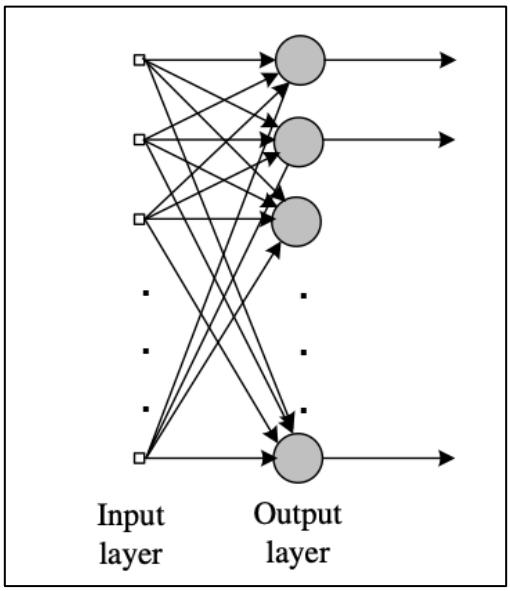

Figure II.5: Feedforward network with a single layer [14].

II.7.2 Multilayer feedforward network

The multilayer feedforward network, illustrated in **Figure II.6**, represents a significant category within neural networks. It comprises an input layer of neurons (source nodes), one or multiple layers of neurons known as hidden layers, and an output layer. Signal propagation occurs sequentially through the network, moving forward layer by layer [14].

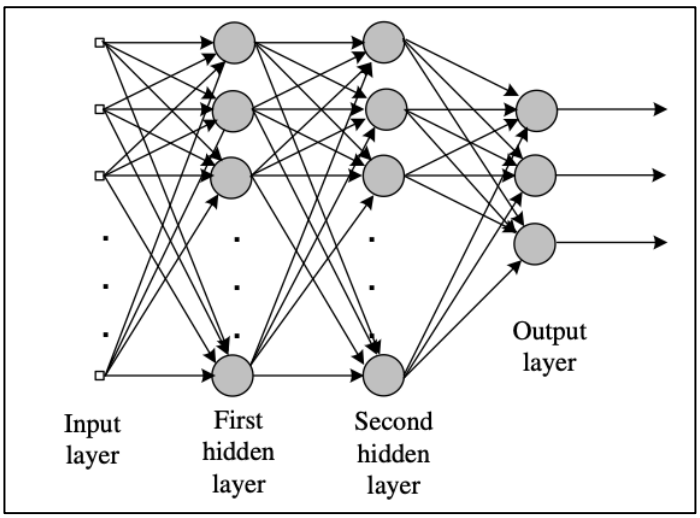

Figure II.6 : Typical feedforward network with two hidden layers and an output layer [14].

II.8 Type of artificial neural networks

There exist diverse types of artificial neural networks, including [15]:

II.8.1 Recurrent neural networks (RNNs)

Are a type of artificial neural network (ANN) characterized by connections between units that create a directed cycle. This cycle forms a sequential pattern, dictating the order of traversal along vertices and edges. RNNs are frequently employed for tasks such as speech and handwriting recognition.

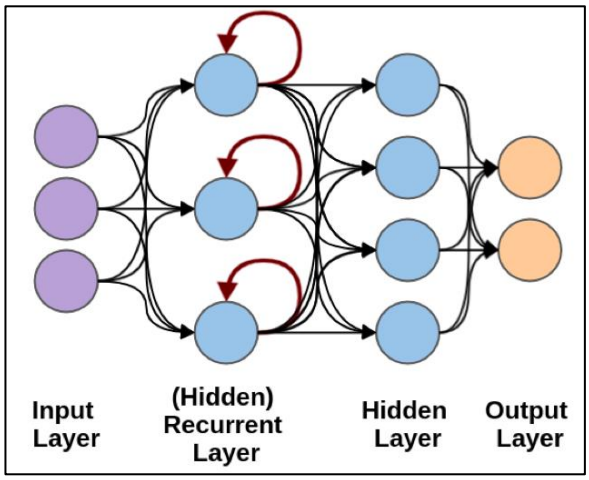

Figure II.7: Recurrent neural network [9].

II.8.2 Modular neural networks

Comprise multiple independent neural networks that operate autonomously without communication or inhibition from other networks during computation.

II.8.3 Feed-forward neural networks (FFNNs)

Are the simplest neural network type, transmitting information in one direction from input nodes to output nodes. They may or may not include hidden layers, making their operation highly interpretable.

II.8.4 Convolutional neural networks (CNNs)

Are among the most widely used models in contemporary applications. They leverage a modified version of the multilayer perceptron, incorporating one or more convolutional layers that can be fully connected or pooled.

II.8.5 De-convolutional neural networks (DCNNs)

Work in the opposite manner to CNNs, aiming to uncover missing signals or features initially considered insignificant to the CNN's task. They utilize a reverse process of the CNN model.

II.9 Machine learning types

Learning algorithms can be categorized into four main types based on the feedback available, representation of learned information, and the presence of prior knowledge. These categories include supervised, unsupervised, semi-supervised, and reinforcement learning, each with its own unique principles and concepts [16].

II.9.1 Supervised learning

Supervised learning relies on labeled input-output training data provided by a trainer to learn a model. The system adjusts its parameters using specific algorithms to produce desired output patterns from given input patterns. However, in application like text processing, video indexing, and bioinformatics, labeled data may be unavailable, costly to generate, or difficult to collect. Additionally, in classification problems, the number of categories may be unknown or may increase with more data. Unsupervised learning systems offer a solution to these challenges by learning from unlabeled data without predefined outputs [16].

II.9.2 Unsupervised learning

Unsupervised learning tackles scenarios where labeled data or guidance from a trainer is absent. Instead, the system learns from unlabeled training data, autonomously adjusting its parameters to uncover meaningful patterns within complex data. Common applications include dimensionality reduction and clustering. However, challenges such as subjective clustering and the difficulty in evaluating results persist. Two proposed solutions are semi-supervised learning, which integrates limited labeled data, and reinforcement learning, which incorporates user feedback to refine the learning process [16].

II.9.3 Semi-supervised learning

Semi-supervised learning bridges the gap between supervised and unsupervised methods, leveraging the strengths of both. It seeks to reduce the need for labeled data in supervised learning while enhancing the outcomes of unsupervised clustering to meet user expectations. This approach relies on assumptions about the labeled and unlabeled data, yet formalizing and verifying these assumptions remains challenging [17].

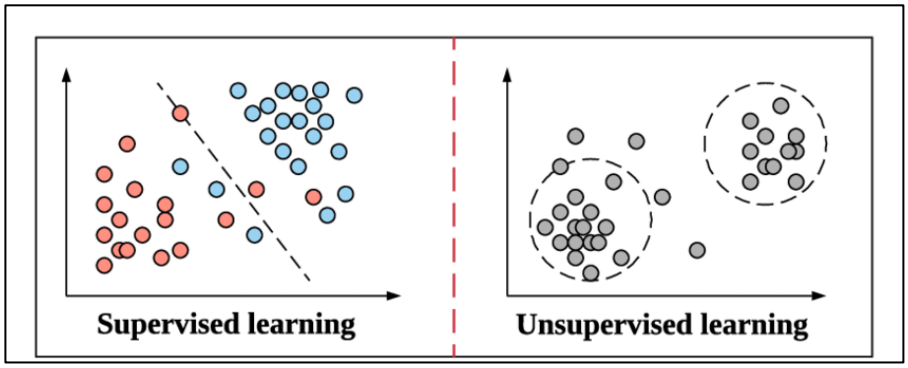

Figure II.8: Examples of Supervised Learning (Linear Regression) and Unsupervised Learning (Clustering) [18].

II.9.4 Reinforcement learning

Reinforcement learning offers an alternative approach to the limitations of supervised and unsupervised learning. Here, the focus shifts to learning through direct interaction with the environment rather than explicit guidance or complete environmental models. In this paradigm, the system receives feedback from its environment, allowing it to discover which actions lead to the most reward through trial and error. Challenges in reinforcement learning include dealing with delayed rewards, where actions impact not only immediate outcomes but also future rewards. Two main strategies for solving reinforcement learning problems exist: searching for effective behaviors through methods like genetic algorithms, or estimating action utilities using statistical and dynamic programming techniques [16].

II.10 Linear and non-linear classification

Linear classification involves assigning data points to discrete classes using a linear combination of their features, while Non-Linear classification deals with separating instances that cannot be linearly separated.

Linear classifiers are preferred for their speed, especially with sparse input data, efficiently classifying large datasets. Conversely, Nonlinear classifiers excel at solving complex problems by identifying patterns that don’t confirm to linear relationships, effectively grouping data points that don’t align along a simple line [19].

II.10.1 Linear classification

Linear classification is the process of classifying a data set into different categories based on a linear combination of the explanatory characteristics of the data set.

Classifiers that use linear function to divide classes include linear discriminant classifiers, Naive Bayes, logistic regression, perceptron, and SVM (linear kernel).

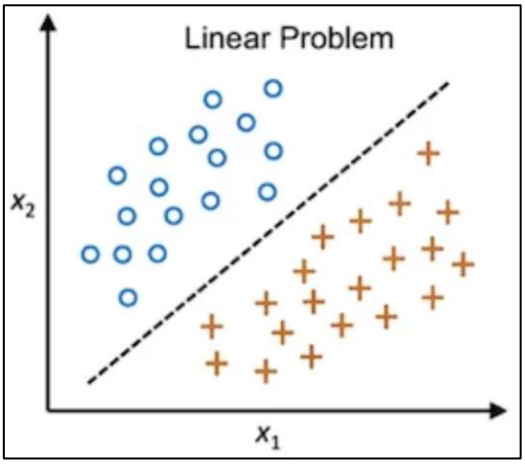

Figure II.9 : Linearly-separable [19].

In the above image, we have two classes namely “O” and “+”. To differentiate between the two classes, draw arbitrary lines to ensure that the two classes are on different sides.

Since we can distinguish one class from another, these classes are said to be “linearly separable”. However, there are countless lines that can be drawn to distinguish these two classes. The exact location of this plane/hyperplane depends on the type of linear classifier.

II.10.2 Non-Linear classification

Nonlinear classification refers to classifying those instances that cannot be linearly separated. Some classifiers that use nonlinear functions for class separation include quadratic discriminant classifiers, multilayer perceptron (MLP), decision trees, random forests, and K-nearest neighbors (KNN).

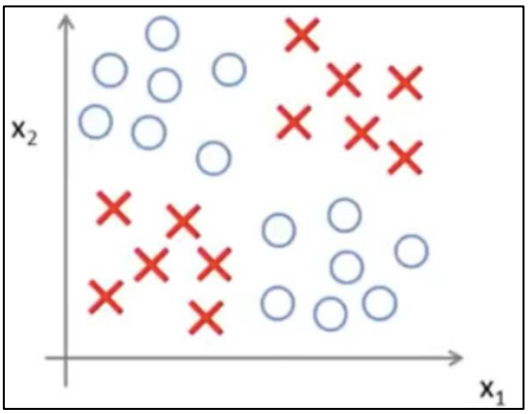

Figure II.10 : Non-linear graph samples example [19].

In the above image, we have two classes namely “O” and “X”. In order to distinguish these two classes, it is not possible to draw any straight line to ensure that the two classes are on different sides. We notice that even if we draw a straight line, there will be points of the first

type between the data points of the second type. In this case, piecewise linear or non-linear classification boundaries are required to differentiate between the two classes.

The main difference is that in the case of Linear classification, data is classified using a hyperplane. In contrast, kernels are used to organize data in the Non-Linear classification case.

II.11 Error Function

An error in machine learning represents the disparity between the anticipated result and the forecasted outcome. It's often expressed simply as:

$$Error = Expected\ Outcome - Predicted\ Outcome \qquad \textbf{(II.7)}$$

The primary goal of a neural network is to determine optimal weight values, achieved when errors are minimized, ideally to zero. This process entails initializing weights, computing neuron outputs using activation functions, error calculation, weight adjustment, and iterative error comparison until the minimum is reached, signifying the network's "learning".

In calculus, finding the minimum point of a function involves location where its first derivative is zero. For neural network training, an error function is crucial to compute this derivative and identify points (weights and biases) where the error is minimized. The choice of error function depends on the model type being trained and is often referred to as a loss function [20].

Error function are categorized into [20]:

- Regression loss function: for predicting continuous outcomes like stock or housing prices.
- Binary classification loss functions: for models predicting two classes, such as cat versus dog or cancer versus no cancer.
- Multiclass classification loss functions: used when predicting more than two classes, as in object detection.

Each category has specific use cases and compatibility with different activation functions, guiding the selection of appropriate error functions for modeling tasks.

II.11.1 Regression loss function

Mean squared error (MSE) loss: Mean Squared Error (MSE) stands out as a favored cost function in ANNs, offering superior performance and widespread adoption compared to other options such as backpropagation. It excels in regression tasks, especially when the target

variable follows a normal or Gaussian distribution. However, its effectiveness diminishes in studies involving multiple variables due to challenges in error comparisons.

$$MSE = \frac{1}{n}\sum_{i=1}^{n}\left(y_i - \hat{y}_i\right)^2 \qquad \textbf{(II.8)}$$

Mean squared logarithmic error (MSLE) loss: The function first calculates the base of the logarithm of predicted values and calculates the mean square error.

Mean absolute error loss: This value is calculated as the average of the absolute differences between expected and predicted values.

II.11.2 Binary classification loss function

Binary cross-entropy: The cross-entropy loss function is the standard choice for binary classification tasks, favored for its effectiveness. It computes a score reflecting the average disparity between actual and predicted probability distributions for predicting class 1. Minimizing this score is the objective, with an ideal cross-entropy value set to 0.

Hinge loss: This function is predominantly utilized to support binary classification based on vector machines.

Squared hinge loss: This function computes the square of the score hinge loss, thereby smoothing the error function's surface and facilitating numerical operations.

II.11.3 Multiclass classification loss function

Multiclass cross-entropy loss: This function is the standard loss function for multiclass classification tasks and is commonly favored over other options. Cross-entropy computes a score that represents the average disparity between the actual and predicted probability distributions for predicting class 1. The goal is to minimize this score, with a perfect cross-entropy value being set to 0.

$$Loss = -\sum_{i=1}^{output\ size} y_i . log\ \hat{y}_i \qquad \textbf{(II.9)}$$

Sparse multiclass cross-entropy loss: This function computes the cross-entropy error without necessity of one-hot encoding the target variable before training.

Kullback-Leibler divergence (KLD) loss: This function quantifies the disparity between a probability distribution and a reference distribution. A KLD loss of 0 indicates identical distributions. It gauges the information loss (in bits) when the predicted probability distribution approximates the desired target probability distribution.

II.12 Optimization algorithms

The primary goal of a neural network is to find the most optimal weights and biases that minimize the loss. Initially the network assigns weights to input connections, which are rarely optimal. The degree of deviation from optimization is measured by the loss. Through an iterative process, the learning algorithm adjusts the weights to minimize the loss function. This process continues until further optimization is not possible. The mathematical function responsible for this optimization is known as the optimization algorithm or optimizer. In the following section, we will delve into some widely-used optimization algorithms, each offering varying levels of accuracy speed, and parallelism [20].

II.12.1 Gradient descent

Gradient descent is an optimization algorithm utilized to minimize the cost function, also known as the loss function, towards zero or the minimum. The cost function, denoted by f(w), is expressed as:

$$f(w) = \frac{1}{N}\sum y_i - w_i x_i \qquad \textbf{(II.10)}$$

Here, y_i represents the known actual value, w_i is the weight corresponding to the feature vector x_i of the i^{th} sample. $w_i x_i$ denotes the predicted value subtracted from the value y_i to compute the error or loss.

In calculus, the first derivative of a function at a particular point yields the slope or gradient of the function at that point. When plotting the cost function f(w), it forms a multidimensional curve (as depicted in **Figure II.11**). The derivative is computed to determine the gradient, indicating the direction along the curve for updating the weights. As the objective is to minimize the cost, the algorithm proceeds in the direction of the negative gradient [20].

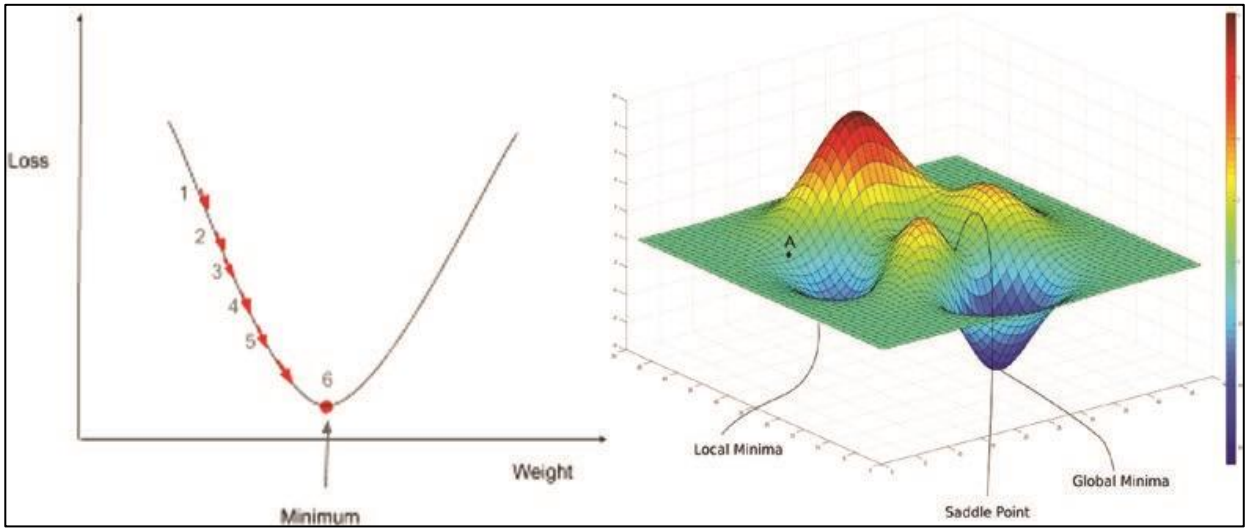

Figure II.11: Cost function with gradient movement toward minimum [20].

In simplified scenario with just one feature, represented by a single weight (w), the cost function resembles the left image in **Figure II.11**.

1. Initially, the algorithm assesses the loss or cost for the initial weights, denoted as f(w), computed at point 1 on the left side of **Figure II.11.**
2. Subsequently, the algorithm determines the gradient (delta) and proceeds downwards along the curve, guided by the negative gradient.
3. While descending, the algorithm calculates the new weights using the formula:

$$weight = weight + alpha * (-delta) = weight - alpha * delta \quad \textbf{(II.11)}$$

Here, alpha termed as the learning rate, dictates the magnitude of steps taken by the gradient to descend the curve towards the minimum point.

The error is recalculated based on the updated weight value, and the process iterates until the algorithm reaches the ultimate minimum cost.

The right image in **Figure II.11** illustrates the error curve for cases where there are multiple weights to optimize. The curve may present multiple apparent minimum points, known as local minima. The goal of the gradient descent algorithm is to identify the global minimum to optimize the weights.

II.12.2 Learning rate

Eq.II.10 introduces the learning rate, denoted as alpha, a critical parameter in the gradient descent algorithm. The learning rate controls the size of steps taken by the algorithm during descent along the curve to find the global minimum. Selecting an appropriate learning rate is crucial. A large learning rate may cause overshooting of the minimum, leading to oscillations and failure to converge. Conversely, a small learning rate requires numerous steps to reach the minimum, resulting in slow convergence. It's important to note that a small learning rate can significantly slow down the learning process.

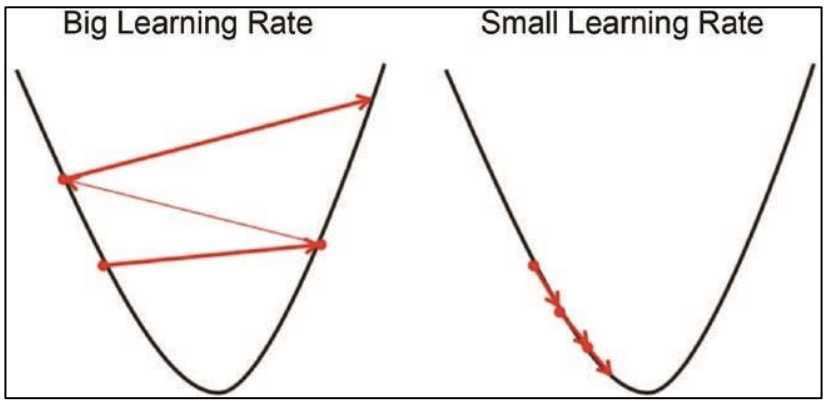

Figure II.12: Effect of big and small learning rates [20].

II.12.3 Adaptive learning rate

In addition to manually setting the learning rate within a practical range, another approach is using adaptive learning rate algorithms. These algorithms dynamically adjust the learning rate during training based on the optimization algorithm's behavior.

One popular adaptive learning rate algorithm is AdaGrad, which adjusts the learning rate for each parameter individually using historical gradients. It provides larger updates for parameters with smaller historical gradients and vice versa, reducing the need for manual tuning.

Another widely used algorithm is Adam, which combines adaptive learning rates with momentum the achieves faster convergence. It adapts learning rates based on past gradients and squared gradients, leading to improved convergence and performance without manual adjustment.

II.12.4 Training algorithms

There are a number of batch training algorithms which can be used to train a network. Here, three types of training algorithms with four training functions each have been evaluated for the classification of lung damage level. They are Gradient Descent algorithms (traingd, traingdm), Conjugate Gradient algorithms (trainscg), and Quasi-Newton algorithms (trainlm) [21].

II.12.4.1 Gradient descent algorithms

Gradient Descent algorithms are among the most widely used training techniques in neural networks. They employ a fundamental gradient descent approach to update weights and biases in the direction opposite to the negative gradient of the performance function.

- **Gradient descent backpropagation algorithm (traingd) :**

This algorithm functions as a gradient descent local search procedure. It computes the output error and adjusts the weights in the direction of the descending gradient of the error.

- **Gradient descent with momentum algorithm (traingdm):**

Gradient Descent with Momentum enhances the traditional gradient descent by incorporating momentum, allowing the network to respond not only to the local gradient but also to recent trends in the error surface. It operates akin to a lowpass filter, enabling the network to disregard small fluctuations in the error surface. Consequently, the inclusion of momentum helps the network overcome the risk of becoming trapped in shallow local minima, facilitating smoother convergence.

II.12.4.2 Conjugate gradient algorithms

Conjugate Gradient algorithms offer an improvement over basic gradient descent by exploring search directions that lead to faster convergence. Unlike traditional gradient descent, which adjusts weights solely along the negative gradient direction, conjugate gradient algorithms search along conjugate directions, resulting in generally faster convergence rates. Despite this advantage, they require only slightly more storage compared to other algorithms, making them suitable for networks with a large number of weights.

- **Scaled Conjugate Gradient (trainscg):**

Scaled Conjugate Gradient stands out for its efficient optimization process. Unlike other conjugate training functions, it doesn't necessitate a line search at each iteration step. Instead, it employs a step size scaling mechanism, eliminating the need for time-consuming line searches and rendering it faster than other second-order algorithms. Although trainscg may require more iterations to converge compared to other conjugate gradient algorithms, it significantly reduces the number of computations in each iteration by omitting the line search process.

II.12.4.3 Quasi-Newton algorithms

Quasi-Newton algorithms represent an advancement over traditional Newton's method and conjugate gradient methods. While Newton's method offers superior optimization and speed, it requires computing the Hessian matrix (second derivatives) of the performance index at the current weight and bias values, making it complex and time-consuming for feedforward neural networks. Quasi-Newton algorithms, inspired by Newton's method but avoiding the need for second derivative calculations, update an approximate Hessian matrix in each iteration, striking a balance between convergence speed and computational complexity.

- **Levenberg-Marquardt backpropagation (trainlm) algorithm:** The levenberg-Marquadt backpropagation algorithm (trainlm) efficiently locates the minimum of a multivariate function expressed as the sum of squares of non-linear real-valued functions. It operates iteratively, ensuring a reduction in the performance function in each iteration, thereby establishing trainlm as the fastest training algorithm for networks of moderate size. However, similar to trainbfg, trainlm incurs memory and computation overhead due to the calculation of the gradient and approximated Hessian matrix.

II.13 Regularization

Regularization is a method utilized in machine learning and statistical modeling to counteract overfitting and enhance a model's ability to generalize. *Overfitting* arises when a model becomes overly complex and starts memorizing the training data, resulting in diminished performance on new, unseen data [20].

The fundamental concept of regularization involves imposing extra constraints or penalties on the model's weights during training. These constraints prompt the model to learn simpler patterns, steering clear of overly intricate or complex relationships within the data.

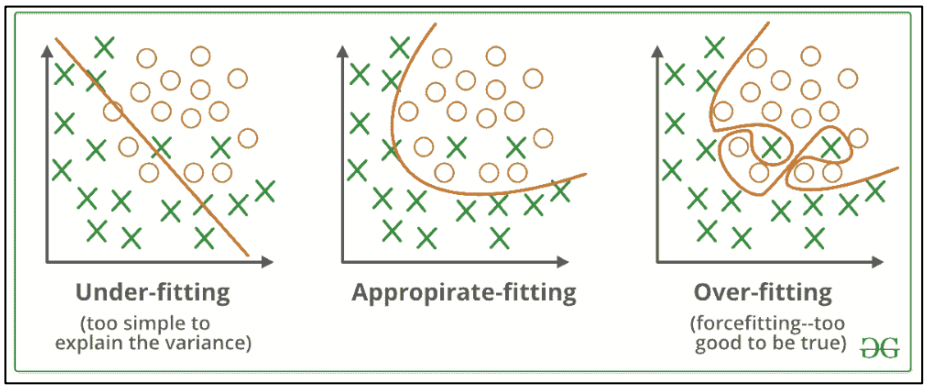

Figure II.13: Classification over- fitting [22].

Under-fitting occurs when a model fails to capture the underlying trend in the training data, resulting in poor fit. This often arises with small or unrepresentative datasets. Underfit models exhibit low accuracy on both training and test sets and should be avoided. To mitigate under-fitting, adding more data or ensuring dataset diversity can help, along with feature engineering to select appropriate features.

II.14 The backpropagation algorithm

The Backpropagation algorithm (BP) stands out as a widely-used method for training feedforward networks, and it falls under the category of supervised learning techniques. It operates through iterative gradient-based techniques to minimize the disparity between the network's actual output and the desired output. Through this process, the algorithm learns from labeled data, adjusting its parameters to improve its ability to make accurate predictions or classifications. The algorithm can be succinctly outlined in the following steps [14]:

1. **Initialization:** All network weights are set to small random values.
2. **Forward Pass:** Input patterns are applied, and outputs are computed. Initially, with random weights, the calculated outputs differ significantly from the desired ones (targets).

3. **Error Calculation:** The discrepancy between the desired and actual outputs is determined for each neuron.
4. **Weight Adjustment:** Using mathematical computations based on the calculated errors, weights are adjusted to reduce errors, bringing neuron outputs closer to their targets. This step is known as the reverse pass.
5. **Iteration:** The process is iterated until the error is minimized.

The BP is associated with serval disadvantages, among which the following are notable:

- Slow convergence: Relative to alternative training algorithms, BP tends to converge slowly. This is attributed to its reliance on gradient descent and its failure to leverage second derivative information to hasten convergence.
- Convergence to a local minimum: Due to its gradient descent nature, BP typically follows the negative gradient direction, leading to convergence at a local minimum of the error surface. As a result, it does not guarantee finding the global minimum, especially in scenarios where the error surface exhibits multiple minima.

II.15 Evaluation metrics

The learned model is an approximation of reality. Therefore, their predictions may be wrong. With a regression model, we can measure the size of the error. The classifier produces a correct or incorrect classification.

In order to evaluate the correctness of the model, we need to choose appropriate evaluation metrics. The evaluation metric quantifies how close the predicted labels given the input data are to the true labels of these observations [23].

Each metric can cover a different aspect of training the model. They can be sensitive to outliers and respect or take into account the distribution of the training data. Some metrics are better suited to subjective labeling, while others are better suited for data that contains outliers that cannot be explained by the data provided. There is no single best metric because which attributes are important depends on the problem [24].

II.15.1 Confusion matrix

The confusion matrix is a widely-used metric in classification tasks, applicable to both binary and multiclass scenarios. **Figure II.14** illustrates an example of a confusion matrix for binary classification.

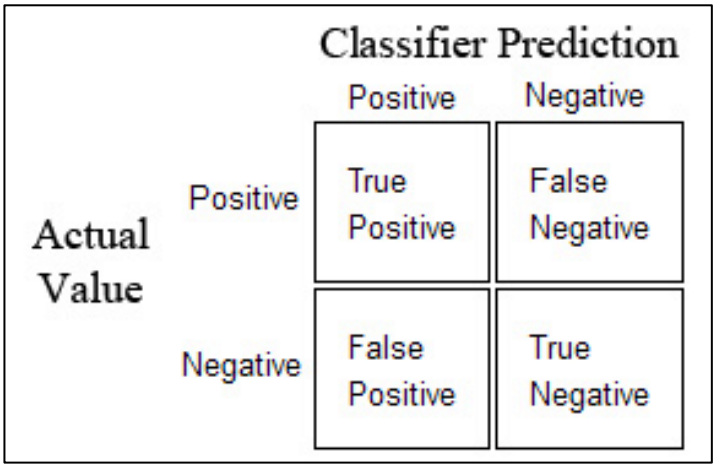

Figure II.14: Confusion matrix example [25].

- **Precision:** Is defined as the ratio of the total number of true positives to the total number of predicted positives. The precision formula is given by:

$$Precision = \frac{TP}{TP+FP} \quad \textbf{(II.12)}$$

- **Recall:** Also known as the true positive rate, is defined as the ratio of the total number of true positives to the total number of actual positives. The recall formula is as follows:

$$Recall = \frac{TP}{TP+FN} \quad \textbf{(II.13)}$$

- **F1 score:** Is a balanced measure that considers both precision and recall when evaluating a model's performance. It addresses the challenge of assessing the model when one metric is significantly smaller than the other. By combining precision and recall into a single metric, the F1 score provides a comprehensive evaluation of the model's quality.

$$F1 = \frac{2\times precicion\times recall}{precision+recall} \quad \textbf{(II.14)}$$

- **Accuracy:** Is the measure of the ratio of correct predictions, both positive and negative, to the total sample size. The accuracy formula is represented as follows:

$$Accuracy = \frac{TP+TN}{TP+TN+FP+FN} \quad \textbf{(II.15)}$$

II.15.2 Receiver operating characteristic (ROC) curve

The ROC curve is an analytical method, represented as a graph, that is used to evaluate the performance of a binary diagnostic classification method. The diagnostic test results need to be classified into one of the clearly defined dichotomous categories, such as the presence or absence of a disease. However, since many test results are presented as continuous or ordinal variables, a reference value (cut-off value) for diagnosis must be set. Whether a disease is present can thus be determined based on the cut-off value. An ROC curve is used for this process, allowing for the assessment of diagnostic accuracy and the determination of optimal cutoff points for decision-making.

II.16 Artificial neural networks application

After years of advancement, neural network theory has made significant strides in various research domains, including pattern recognition, automatic control, signal processing, decision support, and artificial intelligence. The following outlines the current applications of neural networks in several areas [2]:

Pattern recognition: Is the process of describing, identifying, classifying, and interpreting phenomena by analyzing various forms of data. It is grounded in Bayesian probability theory and Shannon's information theory, mirroring the logical processing of the human brain. There are two main methods: statistical and structural pattern recognition. ANNs are commonly used in pattern recognition, gradually replacing traditional methods. Over the years, pattern recognition has advanced significantly and is now widely used in character, speech, fingerprint, remote sensing image, face, and handwriting recognition, as well as industrial fault detection and precise guidance.

Artificial neural network in the field of medicine: Due to the intricate and unpredictable nature of the human body and diseases, the application of Ann is suitable for various aspects such as biological signal detection, analysis, and medical expert systems. In biomedical signal analysis, neural networks excel in handling complex nonlinear relationships and processing continuous waveform data from medical testing equipment. They are particularly useful in EFG signal analysis, auditory evoked potential extraction, EMG and gastrointestinal signal identification, ECG signal compression, and medical image recognition.

Moreover, neural networks provide a solution to the limitations of traditional expert systems by offering nonlinear parallel processing, enhancing knowledge inference, and self-learning abilities. This approach improves efficiency in medical diagnosis and is widely adopted in

anesthesia, critical medicine, and other related fields for tasks like physiological variable analysis, interference signal detection, and clinical condition prediction.

Artificial neural network in the field of transport applications: In recent years, there has been extensive research into applying neural networks to transportation systems. With transportation issues being inherently nonlinear and involving large, complex datasets, neural networks offer significant advantages in addressing these challenges, Their application span various areas such as driver behavior simulation, parameter estimation, pavement maintenance, vehicle detection and classification, traffic pattern analysis, cargo operation management, traffic flow forecasting, transportation strategy, and economy, among others. These applications have shown promising results across multiple domains including air transportation, ship navigation, subway operations, and traffic control.

Artificial neural network in the field of economic: ANNs excel in predicting price changes by analyzing complex market factors such as supply-demand dynamics, household incomes, interest rates, and urbanization levels. They handle incomplete or uncertain data better than traditional statistical methods, leading to more accurate and reliable price trend predictions.

II.17 Conclusion

Finally, this chapter delves into the technical worlds of artificial neural networks and explains their basic concepts, different architectures, and wide range of applications. Inspired by the function of biological neurons, artificial neural networks are composed of interconnected layers of nodes, allowing them to learn complex patterns and perform complex tasks. Using optimization techniques such as the backpropagation algorithm and gradient descent, ANNs can be trained to recognize patterns, classify data, and make predictions with extremely high accuracy. ANNs have been used in various fields, from image recognition to natural language processing, revolutionizing industries and driving innovation. Furthermore, the integration of ANNs with biosensors offers broad prospects for the healthcare and medicine. By leveraging the rich data generated by biosensors, ANNs can enable early disease detection, personalize treatment strategies, and improve patient outcomes.

REFERENCES

[1] J. Abdullah, M. Ahmad, L.Y. Heng, N. Karuppiah, H. Sidek, "*Evaluation of an optical phenolic biosensor signal employing artificial neural networks,* " Sensors and Actuators B: Chemical, Volume 134, Issue 2, Pages 959-965, ISSN 0925-4005, 2008, https://doi.org/10.1016/j.snb.2008.07.009.

[2] Wu, Yc., Feng, Jw. "*Development and Application of Artificial Neural Network.* " Wireless Pers Commun 102, 1645–1656, 2018, https://doi.org/10.1007/s11277-017-5224-x.

[3] A. Abraham, "*129: Artificial Neural Network journal*," Oklahoma State University, Stillwater, OK, USA, 2005.

[4] F. Laurene, "*FONDAMENTALS OF NEURAL NETWORKS: ARCHITECTURES, ALGORITHMS AND APPILCATIONS,* " Internatio. Ed, 1992.

[5] M. AL-MUSHIAA, Z. AOUKLI, "*Fault diagnosis technique in electrical systems by neural networks asynchronous machine* (Master's thesis), " University of Bordj Bou Arreridj, 2022.

[6] Montesinos López, O.A., Montesinos López, A., Crossa, J, "*Fundamentals of Artificial Neural Networks and Deep Learning. In: Multivariate Statistical Machine Learning Methods for Genomic Prediction, "* Springer, Cham, 2022, https://doi.org/10.1007/978-3-030-89010-0_10 .

[7] F. Saadi, "*Nonparametric Regression and Model Selection by Means of Artificial Neural Networks* (Doctoral dissertation). " University of Constantine1, 2022.

[8] B.M. Franco Ortellado, "*Applications of artificial neural networks in three agro-environmental systems: microalgae production, nutritional characterization of soils, and meteorological variables management* (Doctoral dissertation). " University de Valladolid, 2019.

[9] N. Benhalima, "*Classification of banknote fitness by artificial neural networks* (Master's thesis). " IBNKHALDOUN University of Tiaret, 2022.

[10] F. Chabot. "*Fine 2D/3D vehicle analysis by deep neural networks,* " university Clermont Auvergne, France ,2018.

[11] R. M. Ignace. *"Concept detection and automatic annotation of medical images by deep learning, "* University of Antananarivo, 2018.

[12] This Picture was taken from (https://medium.com/@zeeshanmulla/ cost-activation-loss-function-neural-network-deep-learning-what-are-these-91167825a4de) (accessed 20 mars, 2024).

[13] A.K. Jain, J. Mao, K.M. Mohiuddin, "*Artificial neural networks: A tutorial. Computer (3),* " 31–44, 1996.

[14] S. Soualmia, "*Semiconductor parameter extraction using EBIC and Cathodoluminescence* (Doctoral dissertation)," University of Batna, 2012.

[15] TechTarget: https://www.techtarget.com/searchenterpriseai/definition/neural-network?amp=1

[16] L. Atidel, " *MACHINE LEARNING TECHNIQUES FOR IMAGE QUALITY EVALUATION* (doctoral dissertation), " Ecole Nationale Polytechnique, 2012.

[17] Tyler Lu, "*Fundamental Limitations of Semi-Supervised Learning*," Master of Mathematics in Computer Science, Waterloo, Ontario, Canada, 2009.

[18] Orchestrating Development Lifecycle of Machine Learning Based IoT Applications: A Survey - Scientific Figure on ResearchGate. Available from: https://www.researchgate.net/figure/Examples-of-Supervised-Learning-Linear-Regression-and-Unsupervised-Learning_fig3_336550812 (accessed 20 Mars, 2024).

[19] https://www.codingninjas.com/studio/library/linear-vs-non-linear-classification (accessed 01 April, 2024)

[20] S. Ansari, "*Deep Learning and Artificial Neural Networks. In: Building Computer Vision Applications Using Artificial Neural Networks.* " Apress, Berkeley, CA, 2023, https://doi.org/10.1007/978-1-4842-9866-4_5.

[21] B. Sharma & K. Venugopalan, "*Comparison of Neural Network Training Functions for Hematoma Classification in Brain CT Images.* " IOSR Journal of Computer Engineering (IOSR-JCE), 16(1), 31-35. e-ISSN: 2278-0661, p-ISSN: 2278-8727, 2014.

[22] https://www.geeksforgeeks.org/regularization-in-machine-learning/ (accessed 01 April, 2024).

[23] G. James, D. Witten, D et al. " *An Introduction to Statistical Learning: with Applications in R.* " Springer Texts in Statistics, Springer New York, ISBN 9781461471387, 2013.

[24] M. Sokolova, G. Lapalme, "*A systematic analysis of performance measures for classification tasks.* " Information Processing & Management, volume 45, no. 4,pp. 427 – 437, ISSN 0306-4573, 2009, https://doi.org/10.1016/j.ipm.2009.03.002.

[25] Steps Toward a Large-Scale Solar Image Data Analysis to Differentiate Solar Phenomena - Scientific Figure on ResearchGate. Available from: https://www.researchgate.net/figure/Confusion-matrix-example_fig1_256418526 (accessed 3 April, 2024).

CHAPTER III

RESULTS AND DISCUSSIONS

III.1 Introduction

In this chapter, we delve into the design and simulation of a unique MIMO biosensor featuring two split ring resonators (SRRs) with a double circle shape, all integrated onto the same circuit board. These innovative fusion merges metamaterial-based sensors with MIMO technology, enhancing sensitivity and versatility in detecting changes in dielectric properties. Each SRR in the biosensor consists of a ring-shaped resonator with a strategically positioned gap, enabling detection of resonant frequency shifts linked to variations in dielectric properties. Utilizing advanced electromagnetic simulation software, we rigorously simulate and evaluate the behavior of this dual SRR MIMO biosensor, enabling comprehensive modeling, optimization, and sensitivity analysis under diverse conditions.

Additionally, we systematically explore various ANN architectures to augment the biosensor's diagnostic capabilities for classifying lung damage cases. These experiments aim to assess different network configurations' performance in lung damage detection pattern recognition tasks.

By intricately integrating ANN technology with our MIMO biosensor and focusing on simulating and discussing the outcomes derived from each simulation, our aim is to bolster its sensitivity, precision, and dependability in identifying and categorizing varying degrees of lung damage, thereby charting promising pathways for enhanced diagnostic precision in clinical settings.

III.2 Structure of the biosensor

III.2.1 Split ring resonator

This passage outlines the analysis of an SRR and its equivalent circuit. When the rings are close enough for significant coupling, a quasi-static analysis determines the SRR's inductance and capacitance. Excitation by a time-varying magnetic field along the SRR's axis causes electric current to flow across the slot between the rings, resembling a displacement current. The slot acts as a distributed capacitance, contributing to the overall capacitance of the SRR. The equivalent circuit includes the SRR's self-inductance L_S and a total capacitance of C_S. The resonant frequency is given by [1]:

$$f_{SRR} = \frac{1}{2\pi\sqrt{L_S C_S}} \qquad \textbf{(III.1)}$$

as specified by Chinmoy Saha et al.

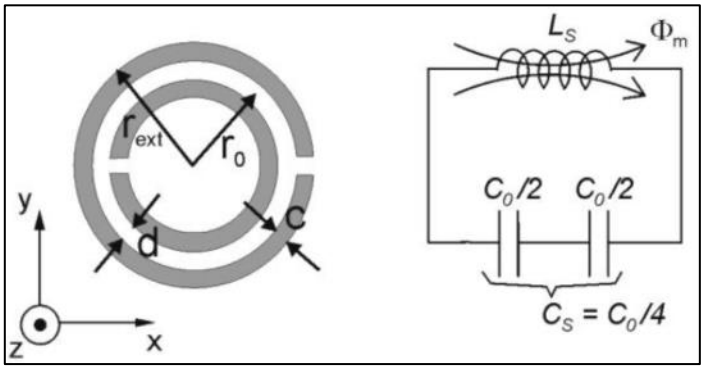

Figure III.1: SRR topology and its equivalent circuit model [1].

III.2.2 Simulated and fabricated MIMO biosensor

The shape of MIMO biosensor structure is as shown in **Figure III.2** a double circle SSR model.

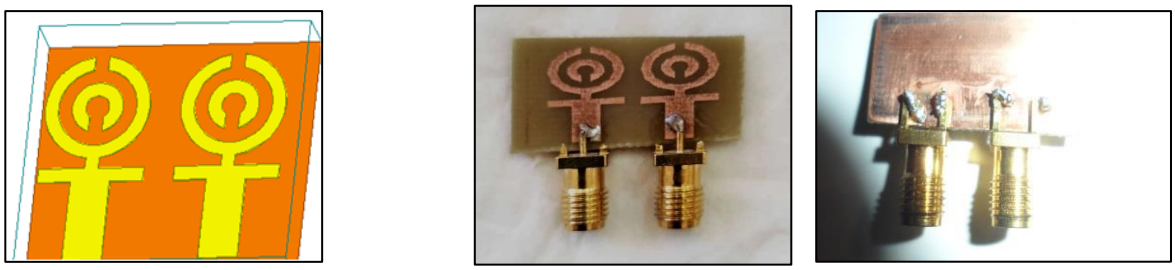

a) Simulated b) Fabricated

Figure III.2: The designed MIMO biosensor**.**

We utilized the parameters listed in the following **Table III.1** to determine the dimensions of our sensor.

Table III.1: Sensor geometries.

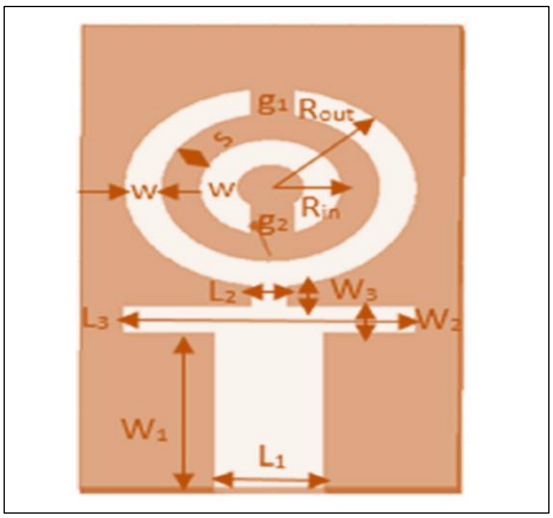

Parameters	Dimensions (mm)
W_1	0.528
W_2	0.105
W_3	0.140
L_1	0.290
L_2	0.09
L_3	0.1
W	0.1
S	0.1
$g_1=g_2$	0.1
R_{out}	0.8
R_{in}	0.4

A lung phantom model with normal and infected tissues was created using simulator to analyze the biosensor performances under conditions such as pneumonia and severe COVID-19 cases. Pneumonia patients, for instance, experience breathing difficulties as their lungs fill with fluid and pus. The phantom includes layers of skin, fat, muscle, water, and lung tissue to evaluate the effectiveness of the biosensor MIMO in detecting fluid in the lungs. **Table III.2** below presents the permittivity, conductivity, density, thermal conductance, and other relevant characteristics, computed using reference [2].

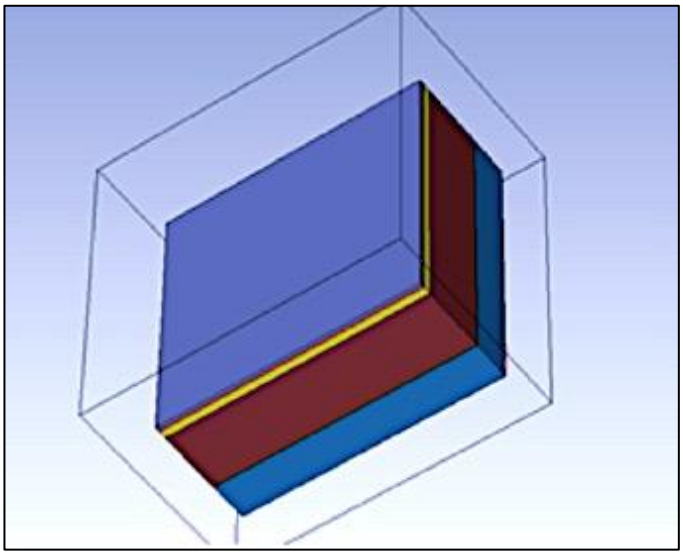

Figure III.3: Designed normal lung phantom model [3].

Table III.2: Parameter values of lung phantoms for 38 GHz measurement [2].

Tissue / Properties	Skin	Fat	Muscle	Lung	Water
Permittivity	12.29	3.44	19.07	7.44	78
Conductivity (s/m)	31.04	2.14	41.82	14.839	1.59
Density (kg/m^3)	1100	910	1041	1020	944
Thermal conductance (W/K/Kg)	0.50	0.24	0.56	0.48	0.60
Heat capacity (Kj/K/Kg)	3.5	2.5	3.7	3.8	4.2
Diffusivity (m^2/s)	$7.6\ 10^{-08}$	$8.8\ 10^{-08}$	$1.4\ 10^{-07}$	$1.7\ 10^{-07}$	-
Blood flow (W/K/m^3)	9100	1700	2700	9500	-
Metabolic rate (W/m^3)	1620	300	480	1700	-
Size	1	3	25	15	1

III.3 Classification of five classes detected of the damage lungs

This study aims to develop a robust model utilizing a MIMO antenna-based biosensor for accurate classification between healthy and damaged lungs with varying water percentages. Our simulation involves categorizing lung conditions into five distinct classes, each representing different levels lung of damage, ranging from 0% to 80% water content, as delineated in **Table III.3**. Additionally, the dataset comprises 500 static samples. Each sample contains five elements representing the five distinct lung damage classes, along with a test from each class, as depicted in **Figure III.4.**

The success of our MIMO antenna-based biosensor classification relies on accurately interpreting the frequency shifts associated with different water percentages within the lung. Ultimately, our objective is to develop a valuable diagnostic tool for precise medical assessments.

Table III.3: Frequency ranges corresponding to each lung classes.

Classes	Frequency Range (GHz)
Healthy lung (0% water)	$37.5 < f_0 < 37.68$
Damaged lung (20% water)	$36.98 < f_0 < 37.4$
Damaged lung (40% water)	$36.90 < f_0 < 36.97$
Damaged lung (60% water)	$36.83 < f_0 < 36.89$
Damaged lung (80% water)	$36.78 < f_0 < 36.82$

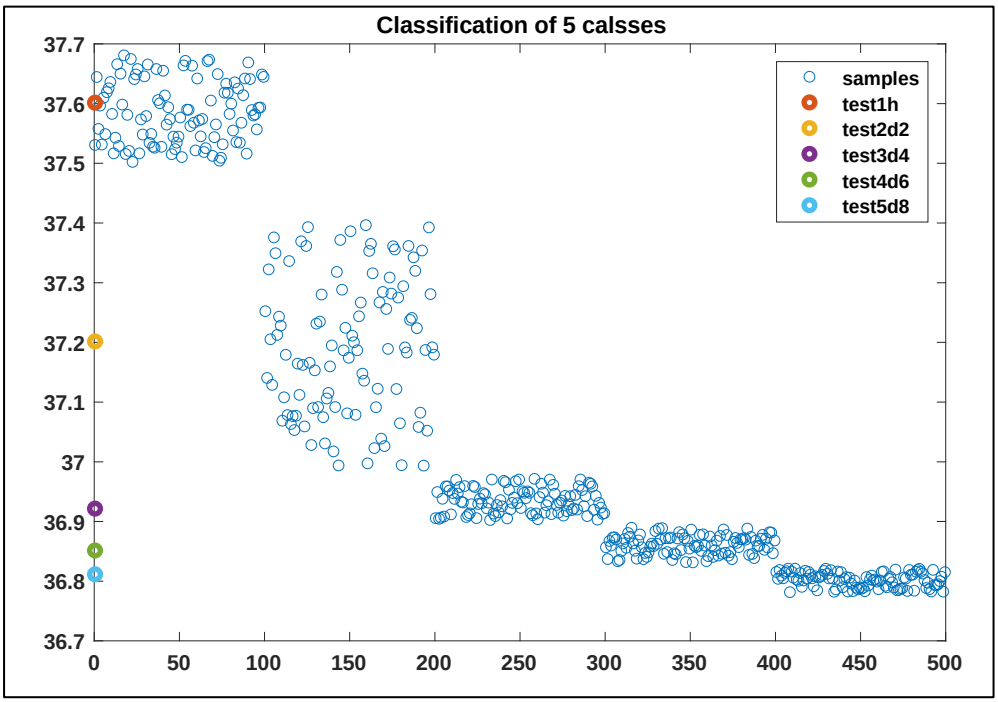

Figure III.4: Classification simulation.

III.4 Designing neural networks with different structures

In our endeavor to enhance the diagnostic capabilities of our biosensor for classifying lung damage cases, we systematically explore various ANN architectures using software. Our future simulation aims to optimize the design and performance of ANNs through systematic parameter variation. By iteratively adjusting parameters, such as the number of neurons and training functions, we aim to develop neural network architectures that maximize classification accuracy while minimizing the risk of overfitting. For the classification task, the neural network undergoes training using 70% of the dataset, consisting of 350 samples, with the remaining 30% reserved for validation and testing, as depicted in **Figure III.5**.

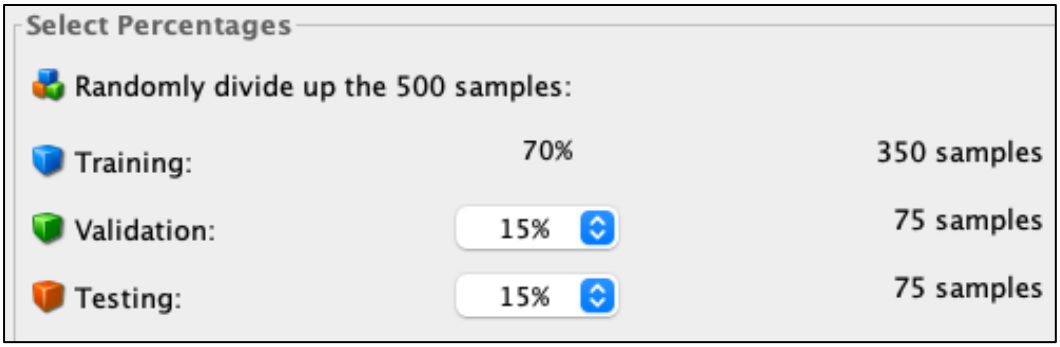

Figure III.5: training, validation and testing percentages.

III.4.1 Analyzing the impact of hidden neuron with Mean Squared Error (MSE)

In the first simulation, we will systematically alter the number of neurons within the hidden layer of our ANN. This deliberate adjustment will be conducted while maintaining other parameters constant. Through this methodical process, we aim to assess the impact of neuron count variations on the network's ability to accurately classify different levels of lung damage. By systematically varying the number of neurons, we can discern the optimal architecture that maximizes the network's performance in lung damage classification. Our performance metric is MSE.

Table III.4: Parameters of Network 1 and Network 2.

Number of trained samples:500		
Network	Network 1	Network 2
Network type	Feed-forward back propagation	
Number of neurons in hidden layer	20	60
Adaption learning function	LEARNGDM	
Performance function	MSE	
Training function	TRAINSCG	
Number of hidden layers	1	1
Activation Function	Layer 1: TANSIG	
Performance	0.037336	0.12267

The **Table III.4** outlines the performance metrics of two neural network configurations, denoted as “network 1” with 20 hidden neurons and “network 2” with 60 hidden neurons. Network 1 achieved a MSE of 0.037336, indicating its proficiency in capturing underlying data patterns. This emphasizes the impact of altering the number of hidden neurons on model performance. Further analysis can delve into understanding the specific patterns captured by each configuration to inform optimal model design.

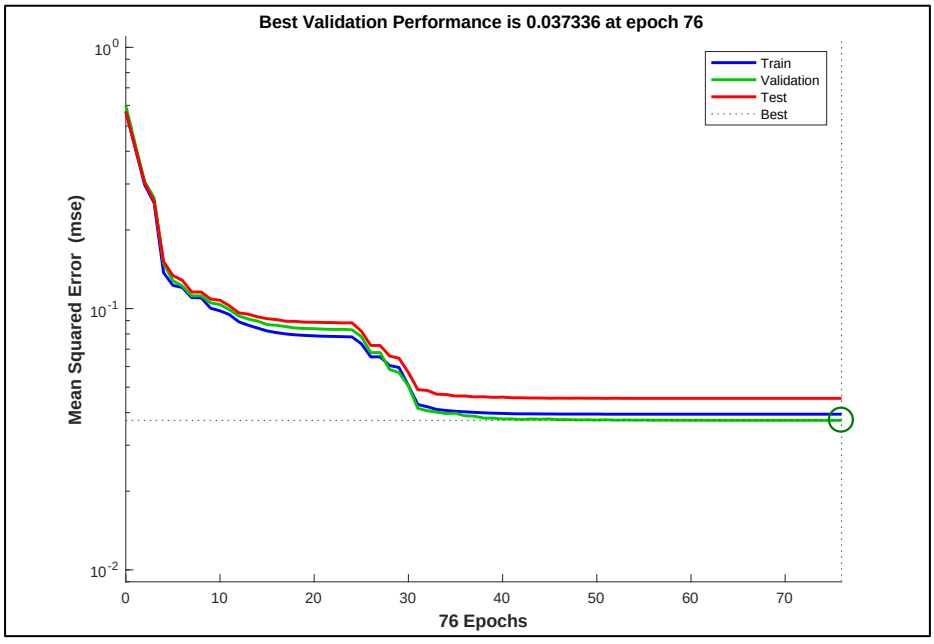

Figure III.6: Best validation performance for Network 1.

III.4.2 Analyzing training functions with Mean Squared Error (MSE)

In this phase, we investigate the impact of different training functions on the performance of our neural network classifier, focusing on accurately classifying lung damage cases. We specifically examine three common functions: TRAINSCG, TRAINGD, and TRAINLM, while maintaining consistency in the number of neurons in the hidden layer. Our performance metric is MSE.

Table III.5: Parameters of Network 3 and Network 4 and Network 5.

Number of trained samples: 500			
Network	Network 3	Network 4	Network 5
Network type	Feed-forward backpropagation		
Training function	TRAINSCG	TRAINGD	TRAINLM
Performance function	MSE		
Number of hidden layers	1	1	1
Number of neurons in hidden layer	20		
Activation function	Layer 1: TANSIG Layer2: SOFTMAX		
Performance	0.23408	0.33304	0.20004

Network 5, trained with the TRAINLM function, achieved the lowest MSE of 0.20004, indicating superior performance in accurately classifying cases. The inclusion of the softmax activation function further enhanced the network's ability to effectively categorize cases. Confusion matrices provide additional insights into classification performance, highlighting Network 5's effectiveness in to a certain accurate categorization.

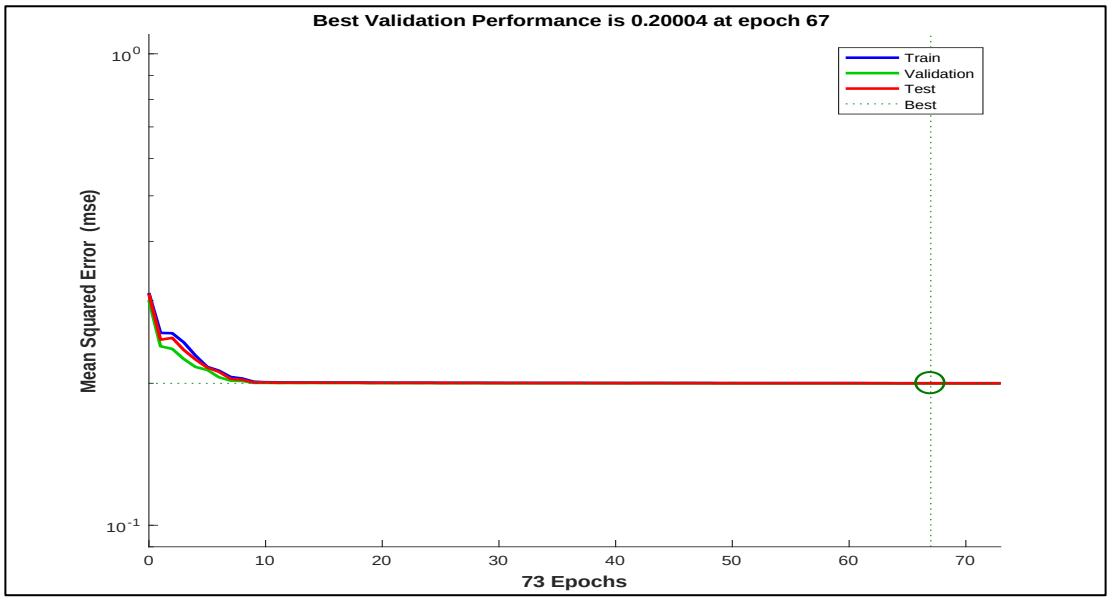

Figure III.7: Best validation performance for Network 5.

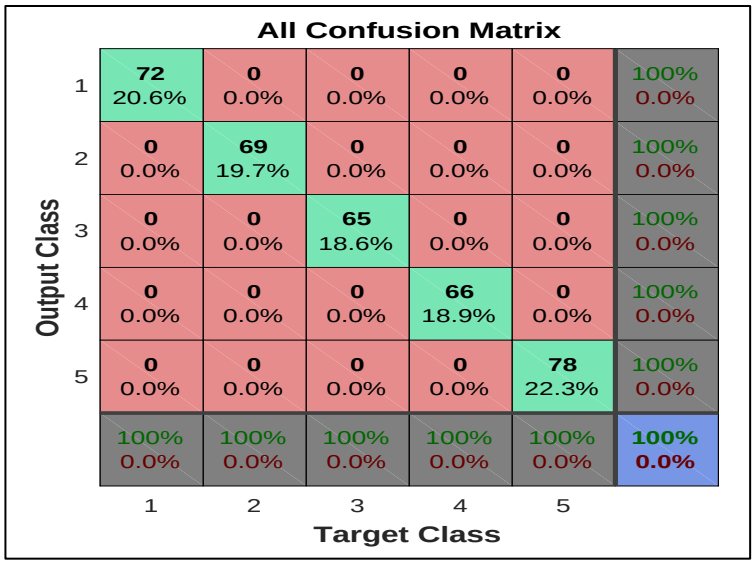

Figure III.8: Confusion Matrix.

III.4.3 Analyzing training functions with Cross-Entropy

In this phase, our objective is to investigate the impact of changing the performance function to Cross-Entropy while keeping all other parameters constant. We systematically vary the performance function to observe its effect on the neural network's performance in classifying lung damage cases. Specifically, we evaluate the network's performance using the TRAINSCG, TRAINGD, and TRAINGDX training functions to determine their influence on classification accuracy.

Table III.6: Parameters of Network 6 and Network 7 and Network 8.

	Number of trained samples: 500		
Network	Network 6	Network 7	Network 8
Network type	Feed-forward backpropagation		
Performance function	CROSS-ENTROPY		
Training function	TRAINSCG	TRAINGD	TRAINGDX
Number of hidden layers	1	1	1
Number of neurons in hidden layer	20	20	20
Activation function	Layer 1: TANSIG Layer 2: SOFTMAX		
Performance	$3.7858\ 10^{-07}$	0.096641	$2.5956\ 10^{-05}$

The results from this phase indicate varying performances among the networks trained with different training functions and Cross-Entropy as the performance function. Notably, Network 6, trained with TRAINSCG, achieved a significantly low performance metric of 3.79 10^{-07}, suggesting high classification accuracy compared to Networks 7 and 8. These findings highlight the superior performance of the TRAINSCG training function when utilized with Cross-Entropy as the performance function. The remarkably low performance metric achieved by Network 6 underscores its high classification accuracy compared to networks trained with TRAINGD and TRAINGDX.

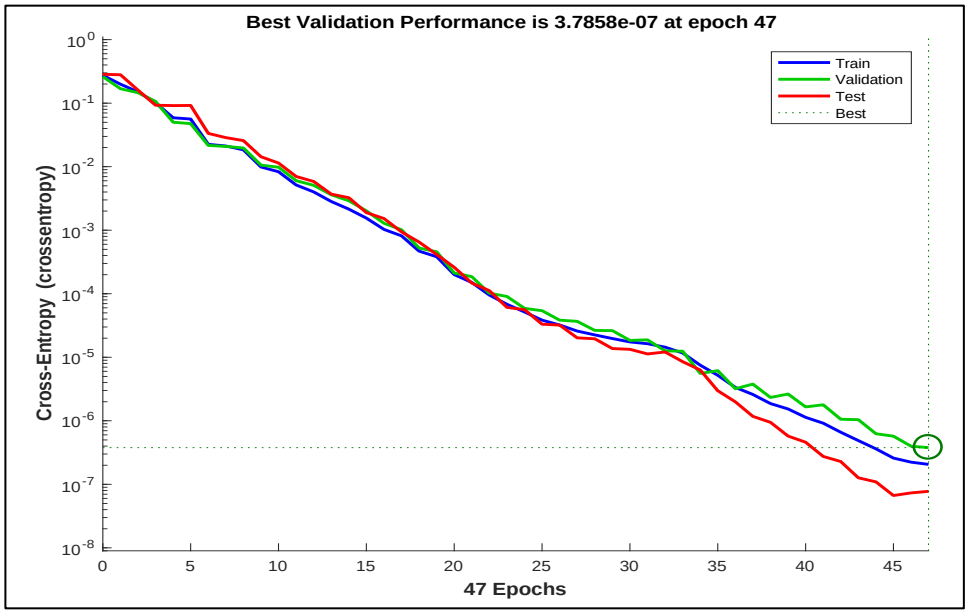

Figure III.9: Best validation performance for Network 6.

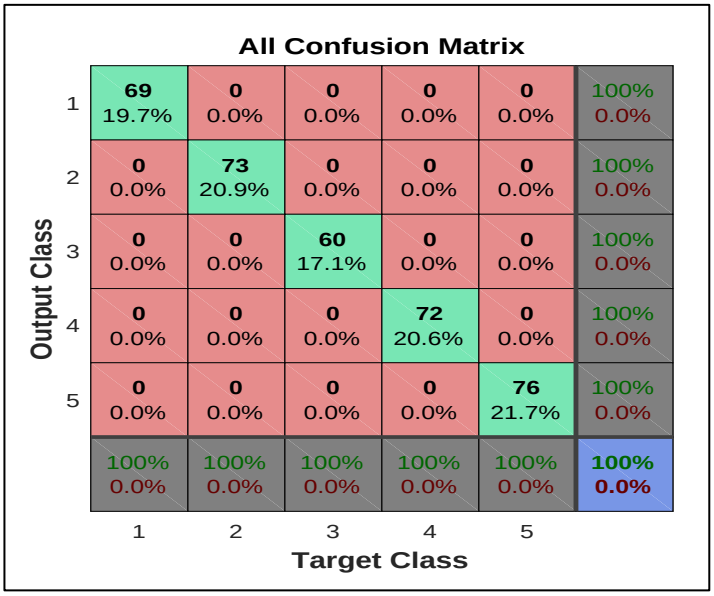

Figure III.10: Confusion Matrix**.**

III.4.4 Analyzing the impact of additional hidden layers

In this phase, we delve into the significance of incorporating an additional hidden layer in the neural network architecture for classifying lung damage cases. Specifically, we examine the performance of two network configurations, Network 9 and Network 10, both featuring a feed-forward backpropagation architecture with two hidden layers.

Table III.7: Parameters of Network 9 and Network 10.

Number of trained samples: 500		
Network	Network 9	Network 10
Network type	Feed-forward backpropagation	
Training function	TRAINSCG	TRAINLM
Performance function	CROSS-ENTROPY	MSE
Number of hidden layers	2	2
Number of neurons in hidden layer	20-20	20-20
Activation function	Layer 1: TANSIG Layer 2: TANSIG Layer 3: SOFTMAX	Layer 1: TANSIG Layer 2: TANSIG Layer 3: SOFTMAX
Performance	$1.1596\ 10^{-07}$	0.2

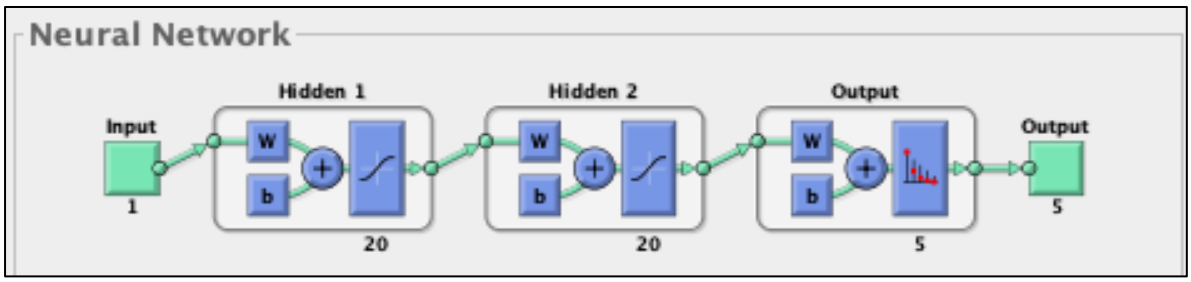

Figure III.11: Architecture of Network 9 and Network 10.

Upon comparison between Network 9 and Network 10, it's apparent that Network 9, trained with the TRAINSCG function, demonstrated superior performance in classifying lung damage cases. Despite both networks sharing identical architectural configurations and utilizing two hidden layers, Network 9 achieved a significantly lower cross-entropy of $1.16\ 10^{-07}$. Remarkably, the inclusion of the hidden layer in Network 9 enhanced its performance when using the CROSS-ENTROPY function compared to previous results. However, this addition had no notable effect on MSE performance.

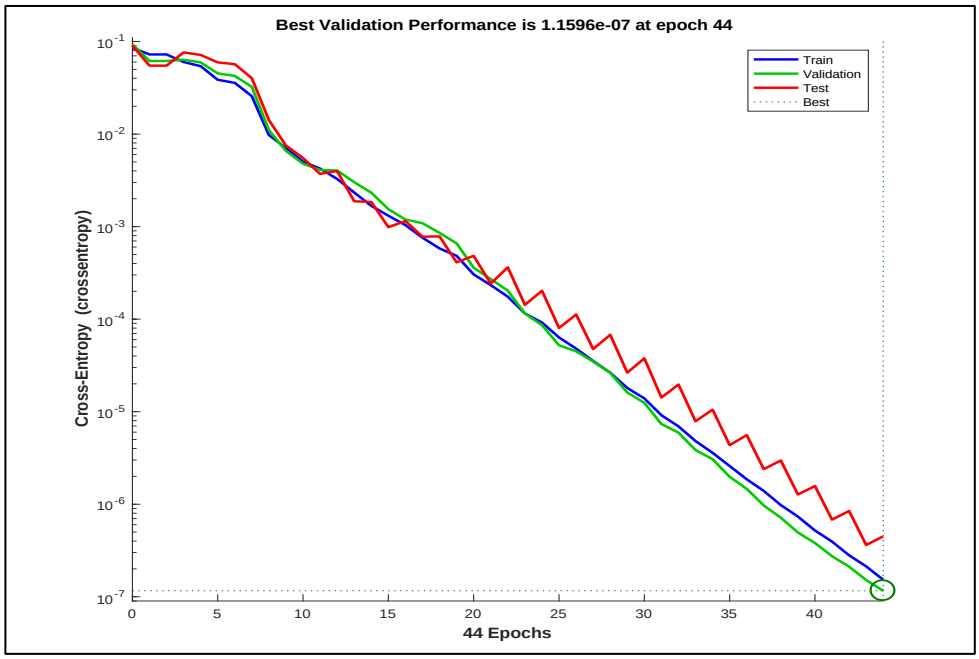

Figure III.12: Best validation performance for Network 9.

III.5 Conclusion for the best structure (high performance)

In the last simulation, after rigorous experimentation and analysis, we have identified the best-performing neural network structure for classifying lung damage cases. We constructed a two-layer feed-forward network with sigmoid hidden and softmax output neurons. This architecture has demonstrated exceptional classification capabilities, achieving high accuracy in categorizing lung damage levels. The network was trained using the scaled conjugate gradient backpropagation algorithm (TRAINSCG), which proved effective in optimizing its performance. The performance metric utilized was the cross-entropy function, which provided valuable insights into the network's accuracy and efficiency.

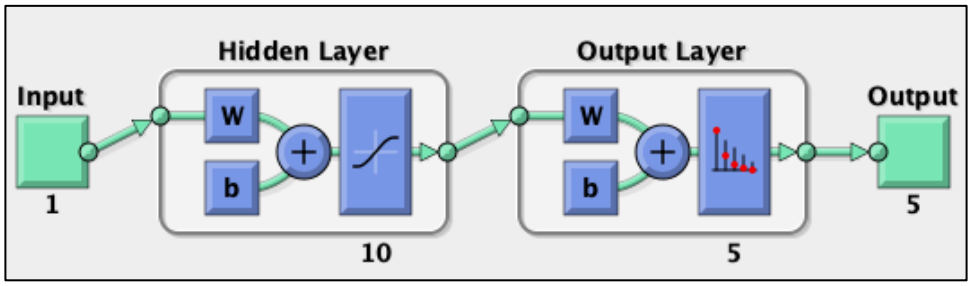

Figure III.13: Architecture of Network 11.

Table III.8: Parameters of Network 11.

Number of trained samples:500	
Network	Network 11
Network type	Feed-forward back propagation
Number of neurons in hidden layer	10
Performance function	CROSS-ENTROPY
Training function	TRAINSCG
Number of hidden layers	1
Activation Function	Layer 1: Sigmoid Layer 2: SOFTMAX
Performance	8.1139 10^{-08}

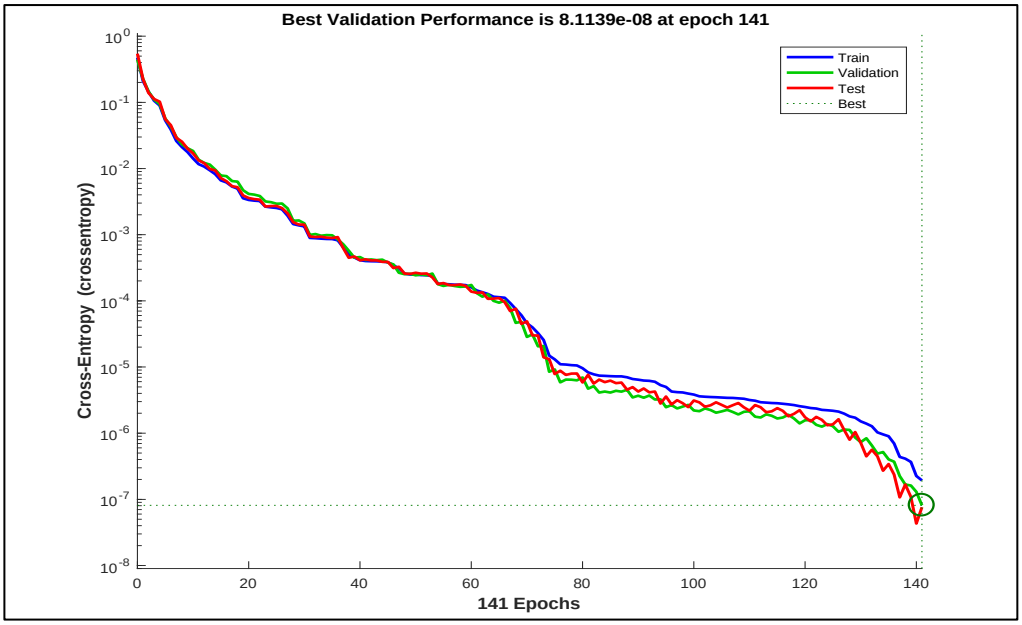

Figure III.14: Best validation performance for Network 11.

In Network 11, featuring a single hidden layer comprising 10 neurons, the utilization of sigmoid activation functions played a crucial role in striking a balance between complexity and performance. This architecture effectively captured the intricate patterns inherent in lung damage classification while mitigating concerns of overfitting and computational complexity. The notable performance metric, indicated by the low cross-entropy value of 8.114 10^{-08}, underscores the network's remarkable accuracy in categorizing lung damage cases. This minimal cross-entropy value signifies reduced uncertainty in the network's predictions, further validating its reliability and effectiveness in real-world applications.

To further evaluate the performance of Network 11 in classifying lung damage cases, **Table III.9** and **Table III.10** below presents the classification probabilities for a subset of patients. This table includes data from 15 patients, with different samples from each of the five lung condition classes: Healthy lung (**0% water**), Damaged lung (**20% water**), Damaged lung (**40% water**), Damaged lung (**60% water**), and Damaged lung (**80% water**). The classification probabilities provide insight into the network's ability to accurately differentiate between varying levels of lung damage across different patients. Analyzing these probabilities allows for a more comprehensive assessment of Network 11's efficacy in real-world applications.

Table III.9: The classification probabilities for Network 11.

patient	37.6	37.50	37.20	37.40	36.92	36.97	36.85	36.83	36.81	36.82
CL 5	5.6174 10^{-23}	1.093 10^{-22}	2.37 10^{-24}	3.2965 10^{-22}	1.2864 10^{-20}	7.2486 10^{-18}	2.1167 10^{-18}	5.9426 10^{-05}	1	0.9999
CL 4	5.0736 10^{-11}	9.4294 10^{-11}	2.1155 10^{-14}	6.2735 10^{-11}	1.1428 10^{-11}	2.8527 10^{-09}	1	0.9999	1.4559 10^{-10}	3.4353 10^{-05}
CL 3	2.089 10^{-10}	1.3996 10^{-11}	1.573 10^{-15}	2.3716 10^{-12}	1	0.9999	5.8846 10^{-17}	3.092 10^{-11}	8.4898 10^{-15}	7.9289 10^{-12}
CL 2	1.986 10^{-09}	5.1902 10^{-08}	1	1	1.2876 10^{-12}	3.867 10^{-05}	2.9503 10^{-16}	3.5508 10^{-10}	1.5972 10^{-13}	1.243 10^{-10}
CL 1	1	1	6.5129 10^{-13}	7.412 10^{-07}	2.7927 10^{-17}	5.202 10^{-13}	6.5913 10^{-21}	2.2646 10^{-15}	2.7782 10^{-19}	3.5512 10^{-16}

Table III.10: The classification probabilities for Network 11.

patient	36.79	36.95	37.30	36.84	37.10	36.87
CL5	1	1.7632 10^{-20}	4.0607 10^{-23}	1.9673 10^{-13}	6.0122 10^{-25}	3.1305 10^{-20}
CL4	8.1906 10^{-14}	4.9643 10^{-12}	4.1843 10^{-12}	1	5.5861 10^{-16}	1
CL3	1.3602 10^{-16}	1	1.8783 10^{-13}	5.833910^{-15}	3.4842 10^{-17}	1.6618 10^{-15}
CL2	2.8524 10^{-15}	3.7943 10^{-11}	1	4.6102 10^{-14}	1	4.3736 10^{-16}
CL1	3.6754 10^{-21}	1.2538 10^{-16}	6.1261 10^{-09}	6.4515 10^{-19}	7.2071 10^{-16}	1.267 10^{-20}

The classification results obtained from the neural network represent a significant milestone in our pursuit of accurately categorizing lung conditions. The provided probabilities offer valuable insights into the model's confidence and precision in its predictions for each class.

Upon scrutinizing the classification probabilities, it becomes evident that the neural network exhibits a remarkable level of certainty in its classifications. For each input sample, one class receives a probability close to unity, indicating a clear and unambiguous prediction. This high level of confidence underscores the effectiveness of the model in discerning between different lung conditions with exceptional precision.

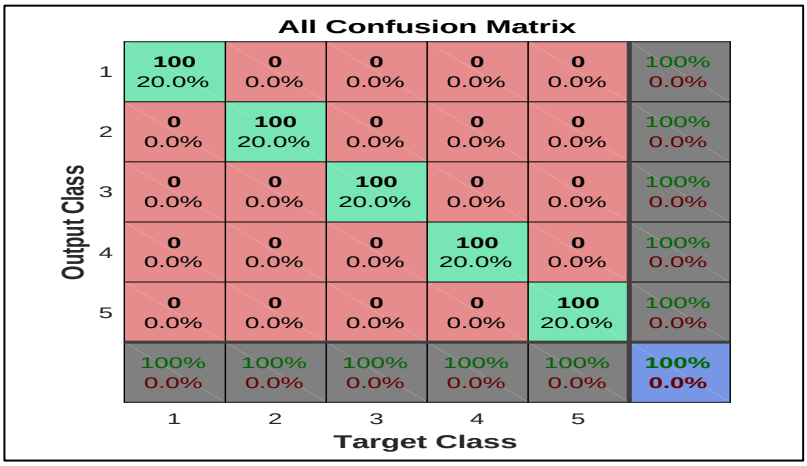

Figure III.15: Confusion Matrix.

The confusion matrix demonstrated the exceptional performance of the ANN, with green squares indicating 100% accuracy across all five lung damage classes. This robustness is highlighted by the absence of false negatives (red squares) and the presence of true positives (blue squares), confirming the network's precise and reliable classification of varying levels of lung damage.

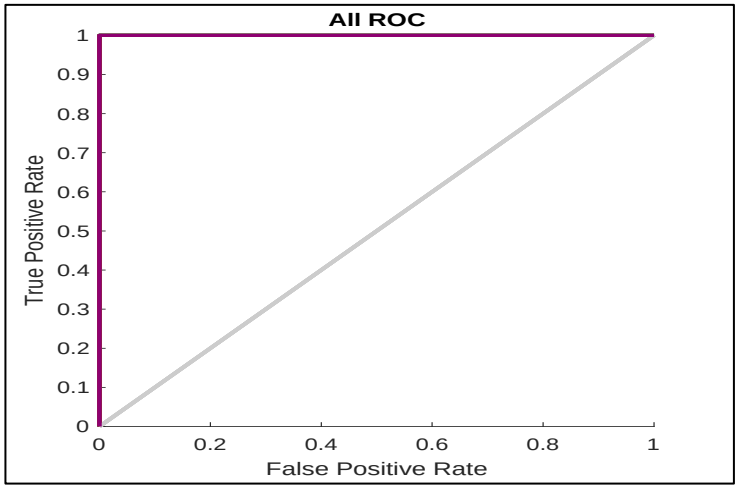

Figure III.16: The ROC curve.

The ROC curve depicts the excellent performance of the model in classifying different levels of lung damage. With the true Positive Rate consistently maximized, the curve illustrates the classifier's strong sensitivity and minimal false negatives. The close proximity to the top-left corner indicates a superior trade-off between true positive rates, emphasizing the model's accuracy in distinguishing between various lung damage classes.

In summation, the outcomes yielded by our neural network are:

- **Precision**: Precision measures the accuracy of positive predictions made by the model. In this case, all classes have a precision score of 1, indicating that all positive predictions made by the model were correct. A precision score of 1 signifies perfect precision, indicating that there were no false positive predictions across all classes.
- **Recall**: Recall, also known as sensitivity, measures the proportion of actual positives that were correctly identified by the model. Similar to precision, all classes have a recall score of 1, indicating that all instances of each class were correctly identified by the model. A recall score of 1 signifies perfect recall, suggesting that there were no false negatives across all classes.
- **F1 Score**: The F1 score is the harmonic mean of precision and recall and provides a balanced assessment of a classifier's performance. In this case, all classes have an F1 score of 1, indicating perfect balance between precision and recall. A score of 1 suggests that there were no false positives or false negatives, resulting in optimal classification performance for all classes.

Overall, these results indicate that the model achieved perfect classification performance across all evaluated metrics, demonstrating its robustness and accuracy in distinguishing between different classes of lung conditions.

III.6 Summary of Architectures and Performance

Below, in the **Table III.11**, we provide a summary of the experimental results obtained from testing various ANN architectures for the detection of lung damage levels. These experiments aimed to assess the performance of different network configurations in a pattern recognition task related to lung damage detection.

Table III.11: Summary of Architectures and performance**.**

Architecture	Performance note
N°1	0.037336
N°2	0.12267
N°3	0.23408
N°4	0.33304
N°5	0.20004
N°6	$3.7858\ 10^{-07}$
N°7	0.096641
N°8	$2.5956\ 10^{-05}$
N°9	$1.1596\ 10^{-07}$
N°10	0.2
N°11	$8.1139\ 10^{-08}$

III.7 Conclusion

In this chapter, our focus was on designing and simulating both the MIMO biosensor with split ring resonators (SRRs) and artificial neural networks (ANNs) for the classification of lung damage levels.

We conducted various simulations to classify the extent of lung damage, adjusting different parameters across multiple network configurations. Through these iterations, we identified the optimal network model, achieving the best performance in the final simulation.

The classification results from the neural network mark a significant milestone in accurately categorizing lung conditions. The probabilities provided by the model offer valuable insights into its confidence and precision in predictions for each class.

REFERENCES

[1] J. D. Baena et al, "*Equivalent-Circuit Models for Split-Ring Resonators and Complementary Split-Ring Resonators Coupled to Planar Transmission Lines*," IEEE Transactions on Microwave Theory and Techniques, vol. 53, no. 4, pp. 1451-1461, May 2005.

[2] A. B. Anwar et al, " *Performance of a 5G MIMO Antenna for Detecting Damaged Lungs of Pneumonia Patients Related to Covid-19*," International Journal of Scientific & Engineering Research, vol. 12, issue 7, ISSN 2229-5518, July 2021.

[3] R. R. Hasan, A. Mortuza S., "*Multiwalled Carbon Nanotube-Based On-Body Patch Antenna for Detecting COVID-19-Affected Lungs*," ACS Omega, vol. 7, no. 32, pp. 28265-28274, 2022.

GENERAL CONCLUSION

This work addresses the vital need for improved diagnostic methods for detecting lung damage, particularly in the context of the COVID-19 pandemic and its long-term health effects. Traditional X-ray methods, though standard, are insufficient for rapid, safe, and efficient diagnosis.

This research introduces a novel split ring resonator (SRR) MIMO biosensor, designed to quickly and safely detect pneumonia associated with COVID-19. Operating within the 5G frequency bands and utilizing advanced metamaterial technology, this compact antenna offers an effective solution for identifying lung abnormalities. By quantifying the water content in the lungs, the integrated MIMO biosensor, combined with the SRR antenna, can accurately discern varying levels of lung damage. Through extensive neural network classification and simulation, we developed a robust model for classifying lung damage, achieving the best performance with the chosen network configuration. This optimal performance underscores the diagnostic capabilities of the proposed antenna system.

Additionally, there is potential to extend the use of this MIMO biosensor system to patients with lung cancer (LC). These patients, already grappling with compromised lung function, are at heightened risk of severe outcomes from COVID-19 due to immunological and inflammatory similarities between lung cancer and COVID-19-related ARDS. Therefore, the proposed system could be invaluable in monitoring and diagnosing complications in such high-risk groups.

However, this research is not without its limitations. The proposed sensor system, although promising in simulations, needs to be tested in real-world conditions to evaluate its practical effectiveness and response. Future research should focus on conducting real-life simulations and clinical trials to validate the sensor's performance and refine its application.

As perspectives, this thesis underscores the significance of innovation and interdisciplinary collaboration in addressing critical healthcare challenges. By harnessing advanced technologies and research endeavors, such as integrating terahertz technology to surpass current millimeter wave capabilities and enhance biosensor precision, we are poised to advance biomedical engineering and significantly impact public health outcomes.

ANNEXES

1) Prototype conception:

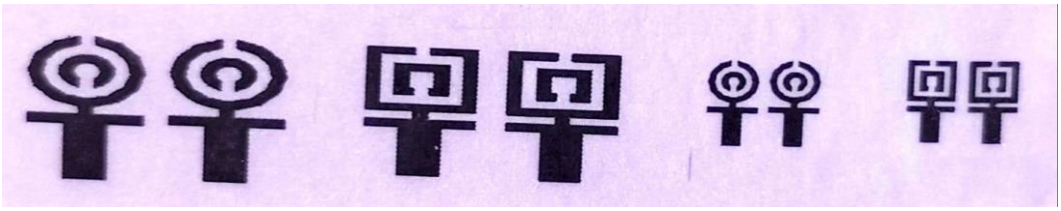

Figure 01: Model of selected MIMO sensors on tracing paper.

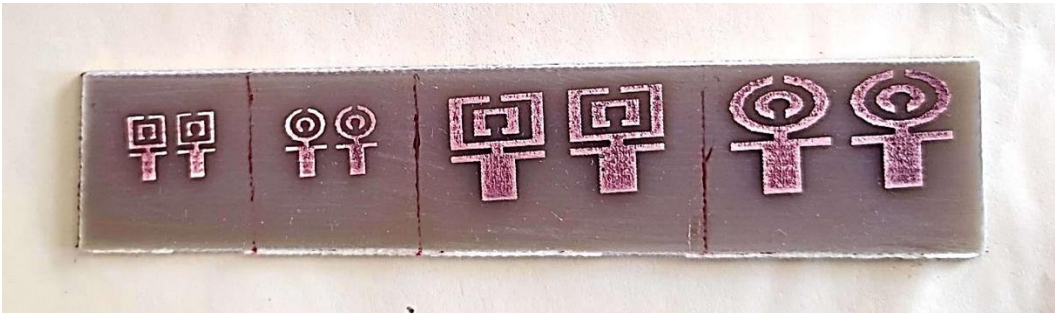

Figure 02: Fabrication of four MIMO sensors (X3 in mm).

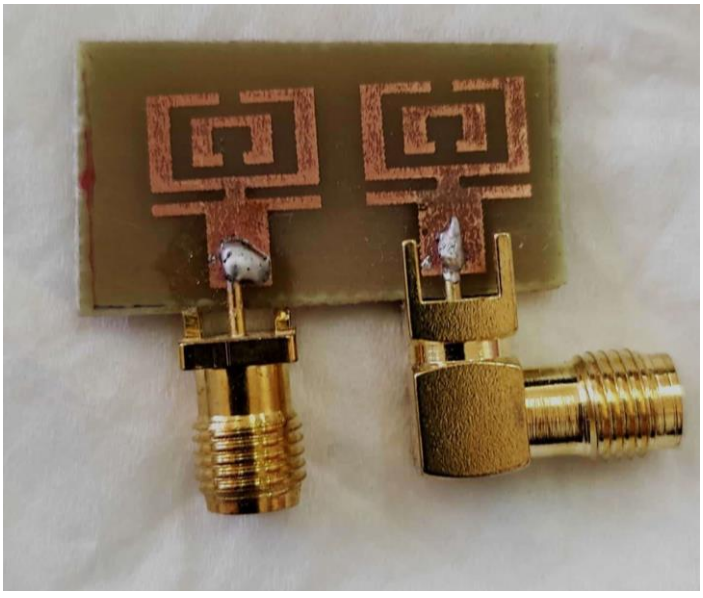

Figure 03: MIMO sensor (model 1: X3 in mm) with ports (front).

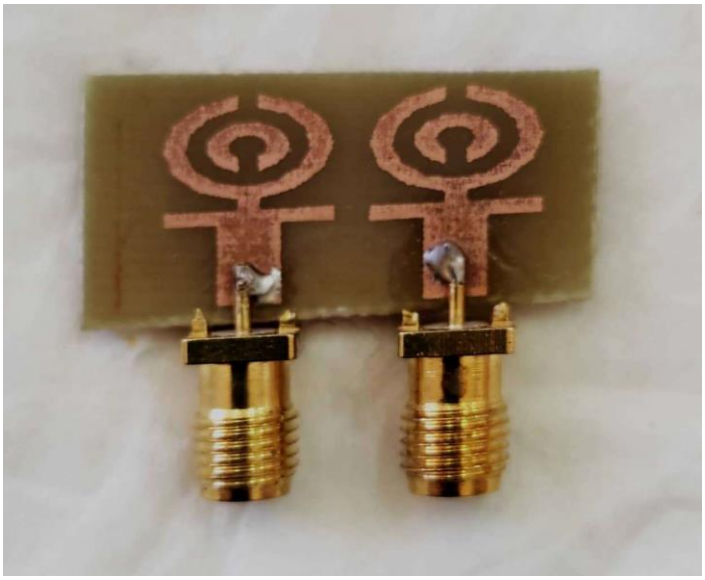

Figure 04: MIMO sensor (model 2: X3 in mm) with ports (front).

2) Soft Word Graphics:

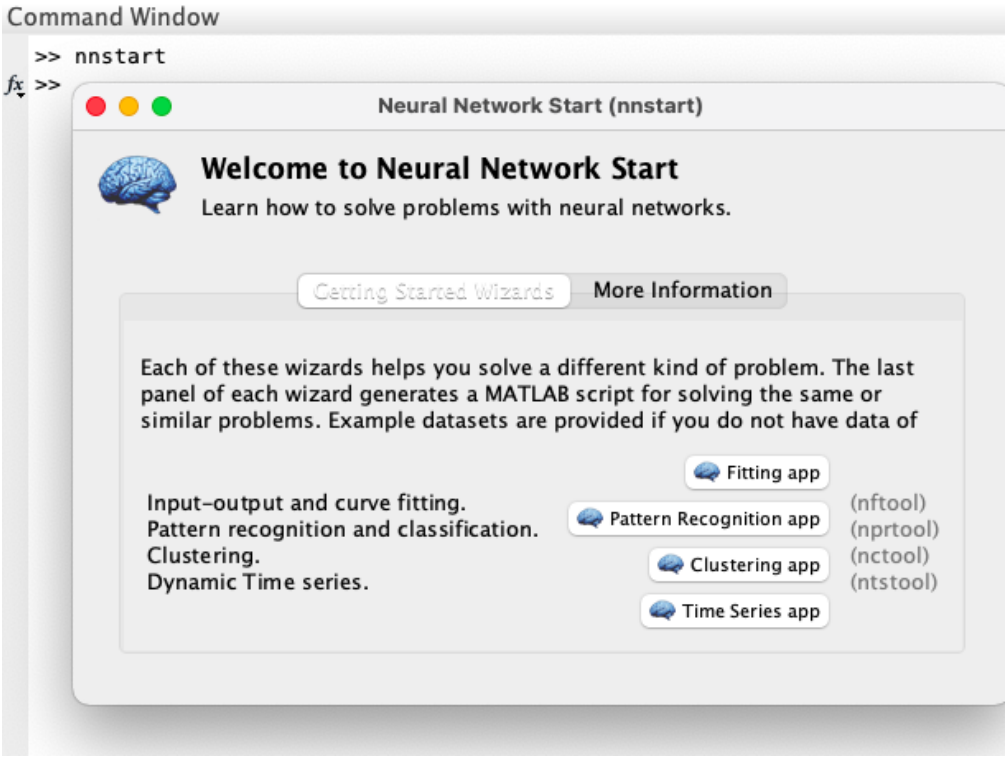

Figure 05: Interface of neural network start.

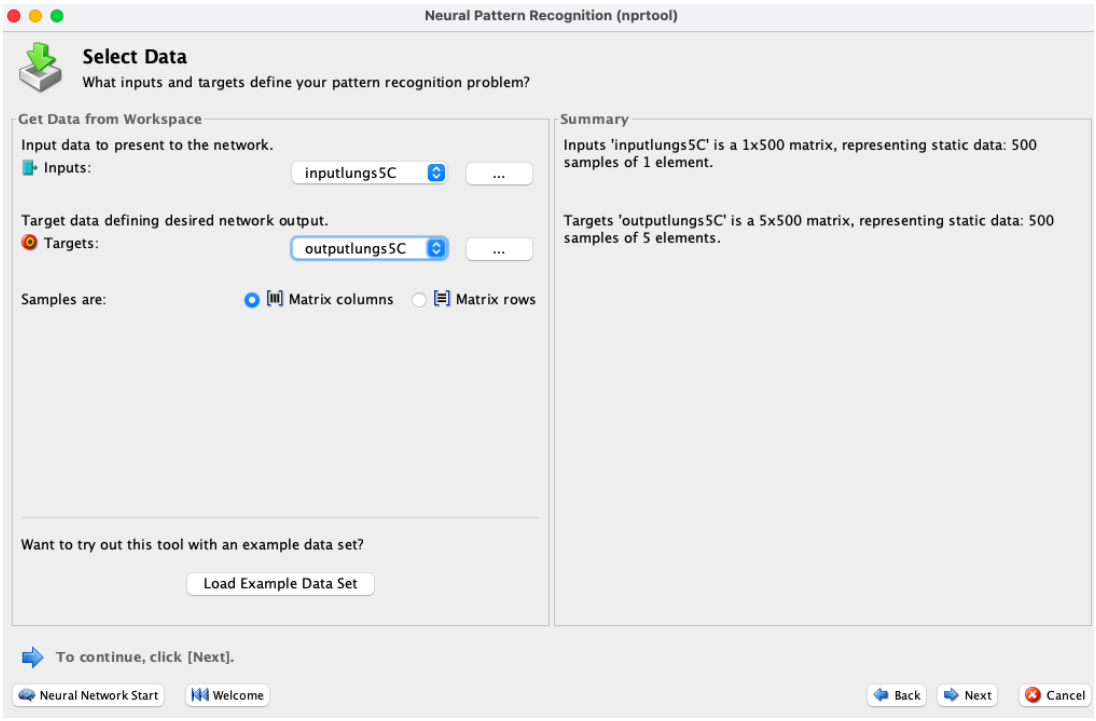

Figure 06: Neural pattern recognition data selection.

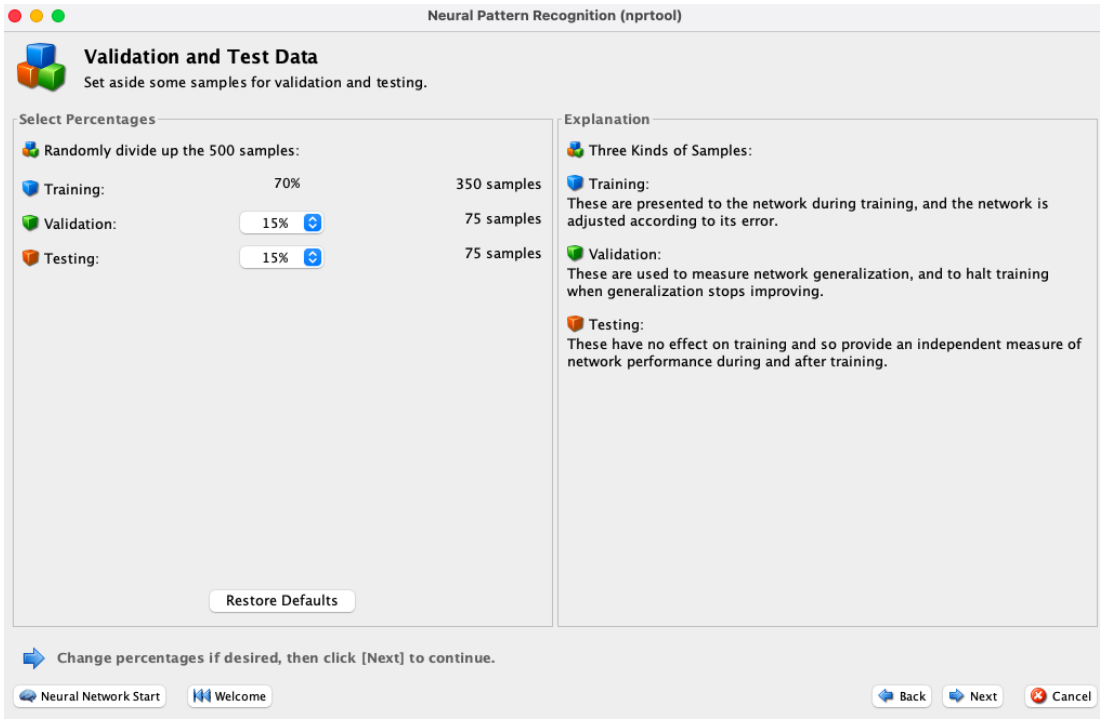

Figure 07: Validation, testing and training percentages.

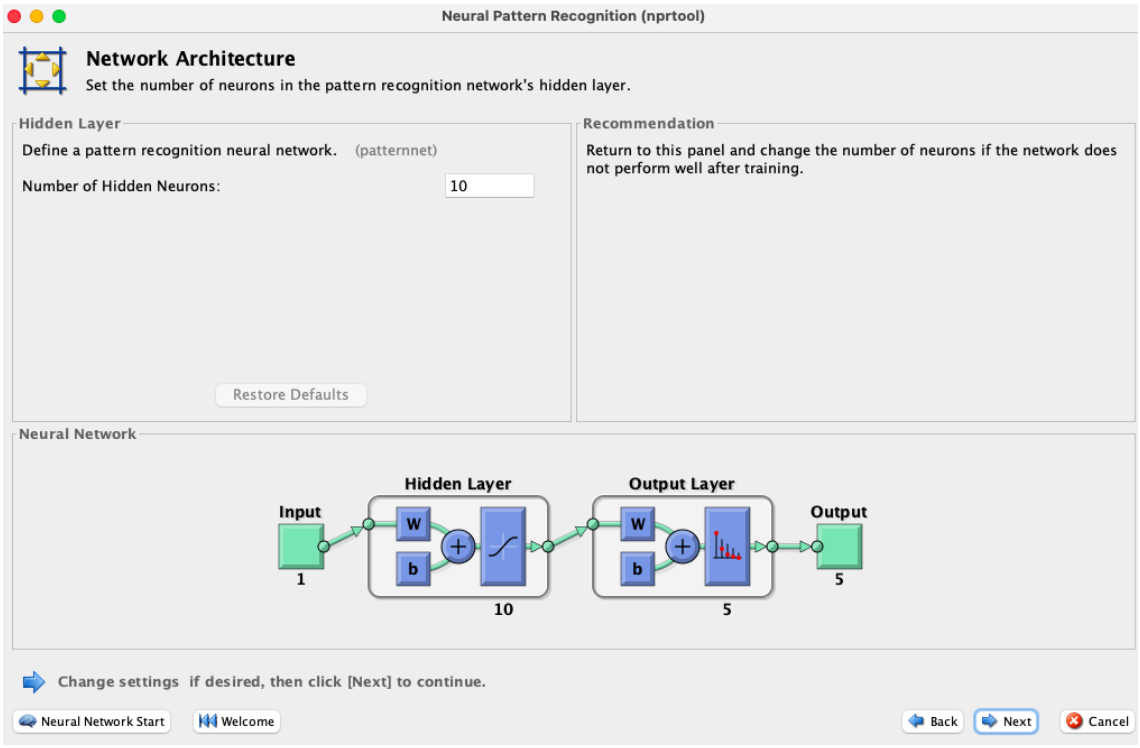

Figure 08: Neural architecture.

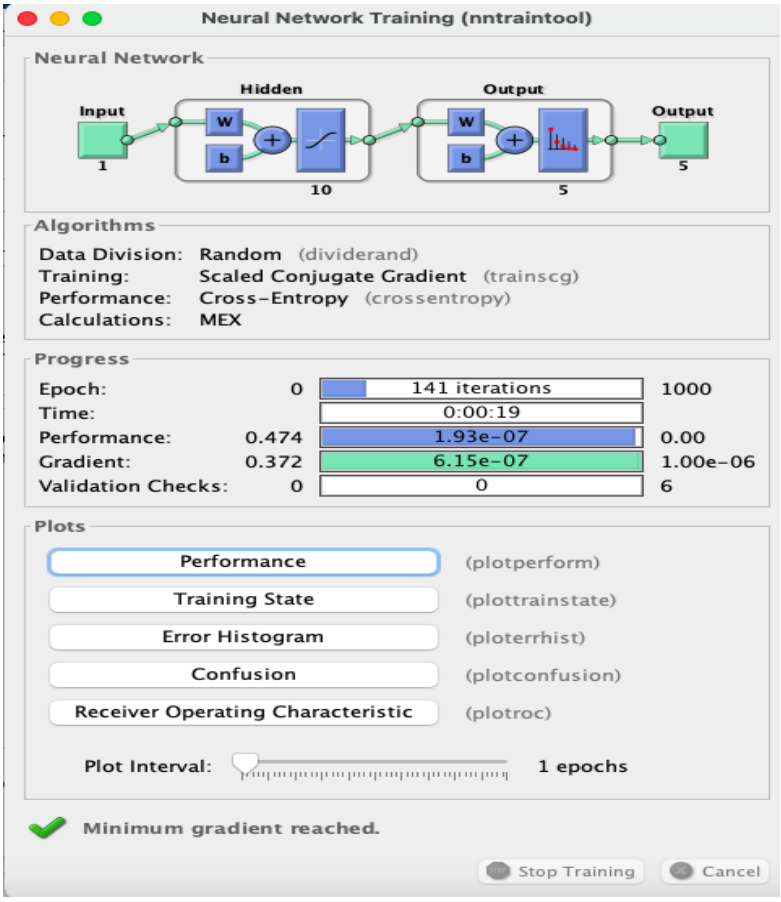

Figure 09: Neural network performance.

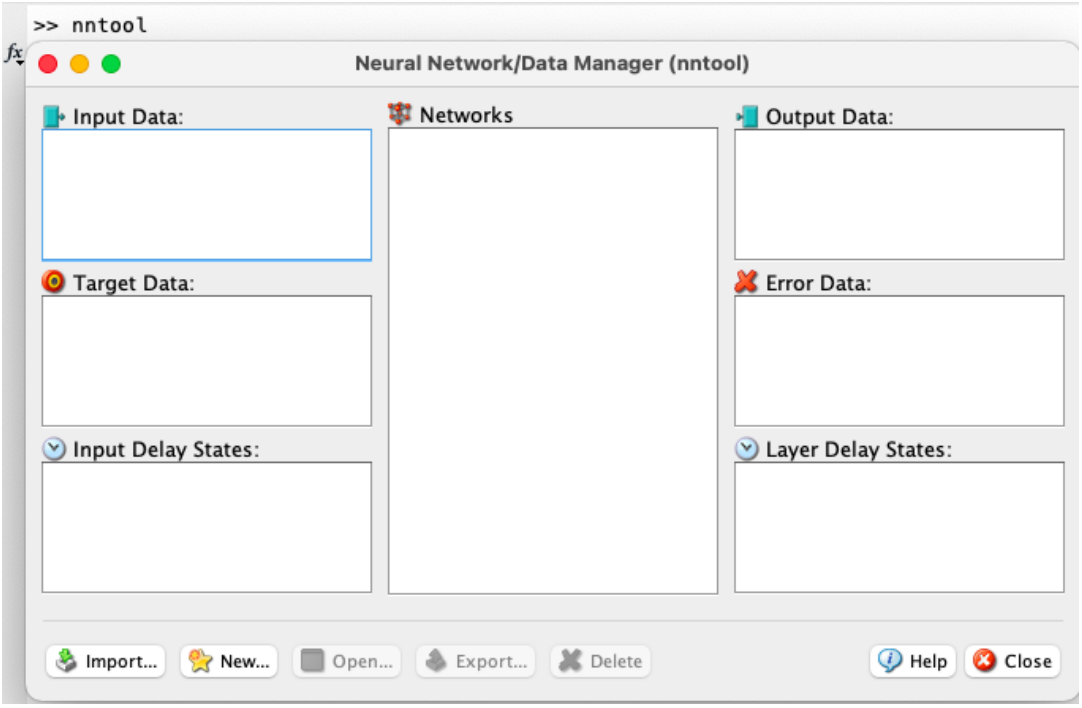

Figure 10: Neural network tool.

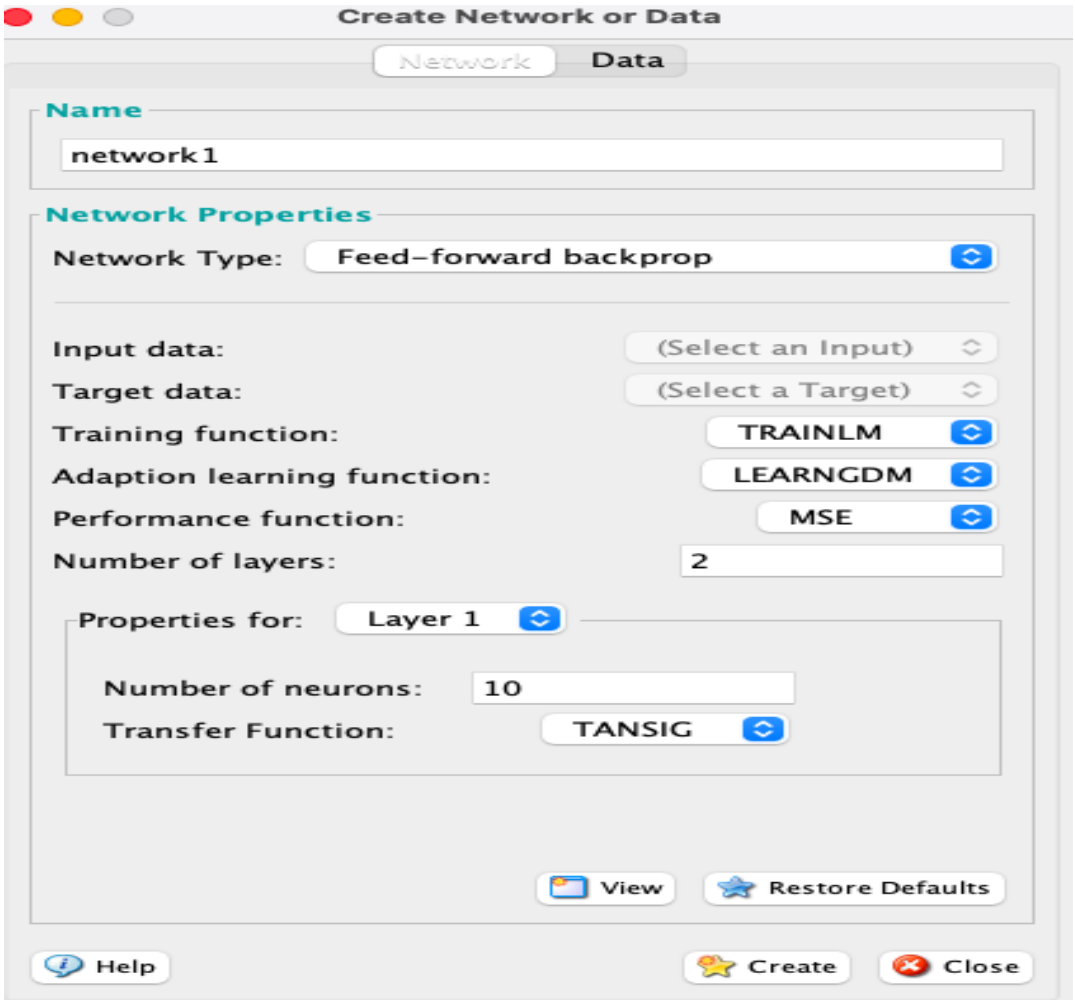

Figure 11: Neural network properties.